

Mathematical Analysis and Design of Parallel RLC Network in Step-down Switching Power Conversion System

Minh Tri Tran^{1,a,*}, Yifei Sun^{1,b}, Noriyuki Oiwa^{1,c}

Yasunori Kobori^{1,d}, Anna Kuwana^{1,e}, and Haruo Kobayashi^{1,f}

¹Division of Electronics and Informatics, Gunma University, 1-5-1 Tenjin-cho, Kiryu 376-8515, Japan

*Corresponding author

^a<t182d002@gunma-u.ac.jp>, ^b<t172d004@gunma-u.ac.jp>, ^c<t14304023@gunma-u.ac.jp>,

^d<kobori@gunma-u.ac.jp>, ^e<kuwana.anna@gunma-u.ac.jp>, ^f<koba@gunma-u.ac.jp>

Keywords: RLC Network, over-under shoot, EMI noise, buck converter, frequency modulation

Abstract. This paper presents a novel circuit design technique and a stability test for an inductor type step-down buck converter. The model of this system is analyzed on both the time and frequency domains. The transfer function and the self-loop function of the power stage are derived and analyzed based on the widened superposition principle. The alternating current conservation technique is proposed to measure the self-loop function. Moreover, the charge and discharge voltages of the capacitor in the RLC of the power stage are analyzed by the energy propagation principle. Therefore, the balanced charge-discharge time condition is written by $T = 2\pi/\omega = 2\pi\sqrt{LC} = 4\pi RC$ if the values of R, L and C are chosen by the relation $|Z_L| = |Z_C| = 2R$. In overdamped case $|Z_L| = |Z_C| < 2R$, the power stage is unstable. The overshoot and undershoot phenomena of this network are improved by a parallel RLC circuit. Furthermore, the electro-magnetic interference noise of the switching control source is flat spread on every operation duty cycle of the control source by a frequency modulation technique. As a result, the step-down switching power network is designed so that the overshoot phenomena is perfectly controlled, the ripple level is very small (lower than 0.05 mV peak to peak), and the spectrum levels are kept below 10 μ V, which is compared to the desired set voltage of 5 V.

1. Introduction

Nowadays, the demand for fully integrated components of a power supply system gives rise to great attention to a single switching system with high efficiency of the energy propagation and low cost of fabrication. The interest of the public is motivated by the great number of functions available on these devices and also by their smaller and smaller sizes [1]. Moreover, the requirements for the time response, the overshoot phenomena and the output voltage ripple of these systems are extremely strict in some applications [2]. Therefore, the design of low-voltage high-efficiency DC-DC buck converter becomes challenging and important research. The applications of the buck converter are switching driver, energy converter, and motor driver systems. In addition, feedback control theories are widely applied in the processing of analogue signals [3].

In conventional analysis of a feedback system, the term of “ $A\beta(s)$ ” is called loop gain when the denominator of the transfer function is simplified as $1+A\beta(s)$, where $A(s)$, $\beta(s)$, are the open loop gain, and feedback gain, respectively. The stability of a feedback network is determined by the magnitude and phase plots of the loop gain. However, a passive filter is not a closed loop system. Furthermore, the denominator of the transfer function of an analog filter, regardless of active or passive is also simplified as $1+L(s)$, where $L(s)$ is called “self-loop function”. Therefore, the term of “self-loop function” is proposed to define $L(s)$ for both cases with and without feedback filters. This paper provides an introduction to the derivation of the transfer function, the measurement of self-loop function and the stability test for the buck converter.

The main contribution of this paper comes from the stability test for the buck converter based on the widened superposition principle and the alternating current conservation measurement. The paper contains a total of 7 sections and 6 appendices. Section 2 constitutes background knowledge, with an explanation of the necessity of network analysis, an essence of the widened superposition principle, an alternating current conversation measurement and a brief presentation of the complex function. Section 3 mathematically analyzes an illustrative second-order denominator complex function considered in details. Section 4 focuses on the time domain and the frequency domain analysis of the power stage of the buck converter. SPICE simulation results for the proposed design of the buck converter are described in Section 5. A brief discussion of the research results is given in Section 6. The main points of this work are summarized in Section 7. We have collected a few important notions and results from analysis in Appendices for easy references.

2. Design considerations for buck converter

2.1. Widened superposition principle

In this section, we propose a new concept of the superposition principle which is useful when we derive the transfer function of a network. The conventional superposition theorem is used to find the solution to linear networks consisting of two or more sources (independent sources, linear dependent sources) that are not in series or parallel. To consider the effects of each source independently requires that sources be removed and replaced without affecting the final result. To remove a voltage source when applying this theorem, the difference in potential between the terminals of the voltage source must be set to zero (short circuit); removing a current source requires that its terminals be opened (open circuit). This procedure is followed for each source in turn, and then the resultant responses are added to determine the true operation of the circuit. There are some limitations of conventional superposition theorem. Superposition cannot be applied to power effects because the power is related to the square of the voltage across a resistor or the current through a resistor. Superposition theorem cannot be applied for non-linear circuit (diodes or transistors). In order to calculate the load current or the load voltage for the several choices of the load resistance of the resistive network, one needs to solve for every source voltage and current, perhaps several times. With the simple circuit, this is fairly easy but in a large circuit this method becomes a painful experience.

In this paper, the nodal analysis on circuits is used to obtain multiple Kirchhoff current law equations. The term of "widened superposition" is proposed to define a general superposition principle which is the standard nodal analysis equation, and simplified for the case when the impedance from node A to ground is infinity and the current injection into node A is 0. In a circuit having more than one independent source, we can consider the effects of all the sources at a time. The widened superposition principle is used to derive the transfer function of a network [4,5,6]. Energy at one place is proportional with their input sources and the resistance distances of transmission spaces. Let $E_A(t)$ be energy at one place of multi-sources $E_i(t)$ which are transmitted on the different resistance distances d_i (R , Z_L , and Z_C in electronic circuits) of the transmission spaces as shown in Fig. 1. Widened superposition principle is defined as

$$E_A(t) \sum_{i=1}^n \frac{1}{d_i} = \sum_{i=1}^n \frac{E_i(t)}{d_i} \quad (1)$$

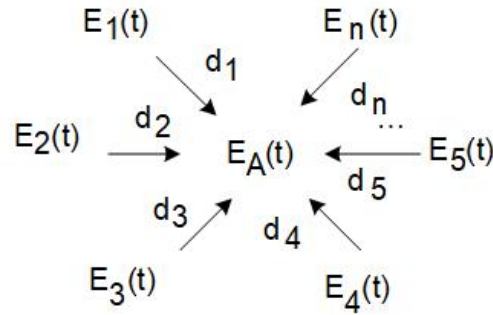


Fig. 1. Energy at one node based on widened superposition principle.

The import of these concepts into circuit theory is relatively new with much recent progress regarding filter theory, analysis and implementation.

2.2. Complex function

In this section, we describe a transfer function as the form of a complex function where the variable is an angular frequency. In frequency domain, the transfer function and the self-loop function of a filter are complex functions. Complex functions are typically represented in two forms: polar or rectangular. The polar form and the rectangular representation of a complex function $H(j\omega)$ is

$$H(j\omega) = \text{Re}\{H(j\omega)\} + j \text{Im}\{H(j\omega)\} = \sqrt{(\text{Re}\{H(j\omega)\})^2 + (\text{Im}\{H(j\omega)\})^2} e^{j \arctan\left(\frac{\text{Im}\{H(j\omega)\}}{\text{Re}\{H(j\omega)\}}\right)} \quad (2)$$

where $\text{Re}\{H(j\omega)\}$ is the real part of $H(j\omega)$ and $\text{Im}\{H(j\omega)\}$ is the imaginary part of $H(j\omega)$, and j is the imaginary operator $j^2 = -1$. The real quantity $\sqrt{(\text{Re}\{H(j\omega)\})^2 + (\text{Im}\{H(j\omega)\})^2}$ is known as the amplitude or magnitude, the real quantity $\arctan\left(\frac{\text{Im}\{H(j\omega)\}}{\text{Re}\{H(j\omega)\}}\right)$ is called the angle $\angle H(j\omega)$, which is the angle between the real axis and $H(j\omega)$. The angle may be expressed in either radians or degrees and real quantity $\frac{\text{Im}\{H(j\omega)\}}{\text{Re}\{H(j\omega)\}}$ is called the argument $\text{Arg}\{H(j\omega)\}$ which is the ratio between the real part and the imaginary part of $H(j\omega)$. The operations of addition, subtraction, multiplication, and division are applied to complex functions in the same manner as that they are to complex numbers. Frequency response of a complex function can be plotted in several ways; three of them are magnitude-angular plots (Bode plots), polar charts (Nyquist charts), and magnitude-argument diagrams (Nichols diagrams). In this paper, the stability test is performed on the magnitude-angular plots and polar chart.

2.3. Graph signal model for complex function

In this section, we describe the graph signal model of a typical complex function which is the same as the graph signal model of a feedback system. A negative-feedback amplifier is an electronic amplifier that subtracts a fraction of its output from its input, so that negative feedback opposes the original signal. The applied negative feedback can improve its performance (gain stability, linearity, frequency response, step response) and reduce sensitivity to parameter variations due to manufacturing or environment. Thanks to these advantages, many amplifiers and control systems use negative feedback. However, the denominator complex functions are also expressed in the graph signal model which is the same as the negative feedback system. A general denominator complex function is rewritten as

$$H(s) = \frac{V_{out}(s)}{V_{in}(s)} = \frac{A(s)}{1 + L(s)} \quad (3)$$

This form is called the standard form of the denominator complex function. The output signal is calculated as

$$V_{out}(s) = A(s) \left[V_{in}(s) - \frac{L(s)}{A(s)} V_{out}(s) \right] \quad (4)$$

Fig. 2 presents the graph signal model of a general denominator complex function. The feedback system is unstable if the closed-loop “gain” goes to infinity, and the circuit can amplify its own oscillation. The condition for oscillation is

$$L(s) = -1 = 1e^{-j\pi(2k+1)}; k \in Z \quad (5)$$

Through the self-loop function, a second-order denominator complex function can be found that is stable or not. The concepts of phase margin and gain margin are used to asset the characteristics of the loop function at unity gain. The conventional test of the loop gain, which is called “Barkhausen’s criteria”, is unity gain and -180° of phase in magnitude-phase plots (Bode plots) [7].

2.4. Alternating current conservation measurement

In this section, we describe a mathematical way to measure the self-loop function based on the alternating current conservation when we inject an alternating signal sources (alternating current or voltage sources) and connect the input of the network into the alternating current ground (AC ground). In general, the term of “alternating current conservation” is proposed to define this technique. The main idea of this method is that the alternating current is conserved. In other words, at the output node the incident alternating current is equal to the transmitted alternating current. If we inject an alternating current source (or alternating voltage source) at the output node, the self-loop function can be derived by ratio of the incident voltage (V_{inc}) and the transmitted voltage (V_{tran}) as shown in Fig. 3. Compared to measurement results of the alternating current conservation with the conventional ones (voltage injection), they are the same.

In order to break the feedback loop without disturbing the signal termination conditions, and ensure that the loop is opened for AC signals, a balun transformer inductor can be used to isolate the signal source from the original network as in Fig. 3(e). In this case, the values of resistors and inductors are very large. Compared to the proposed measurement with the conventional replica measurement, they are the same measurement results [8]. Apply the widened superposition principle at V_{inc} and V_{tran} nodes, the self-loop function is

$$\frac{V_{inc}}{A(s)} = \frac{L(s)}{A(s)} V_{tran} \Rightarrow L(s) = \frac{V_{inc}}{V_{tran}} \quad (6)$$

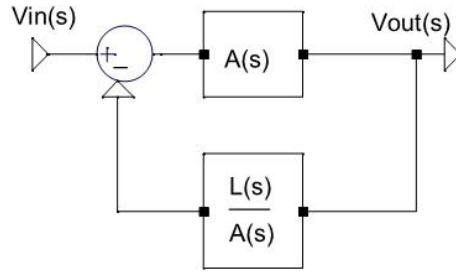


Fig. 2. Signal model graph of general complex function.

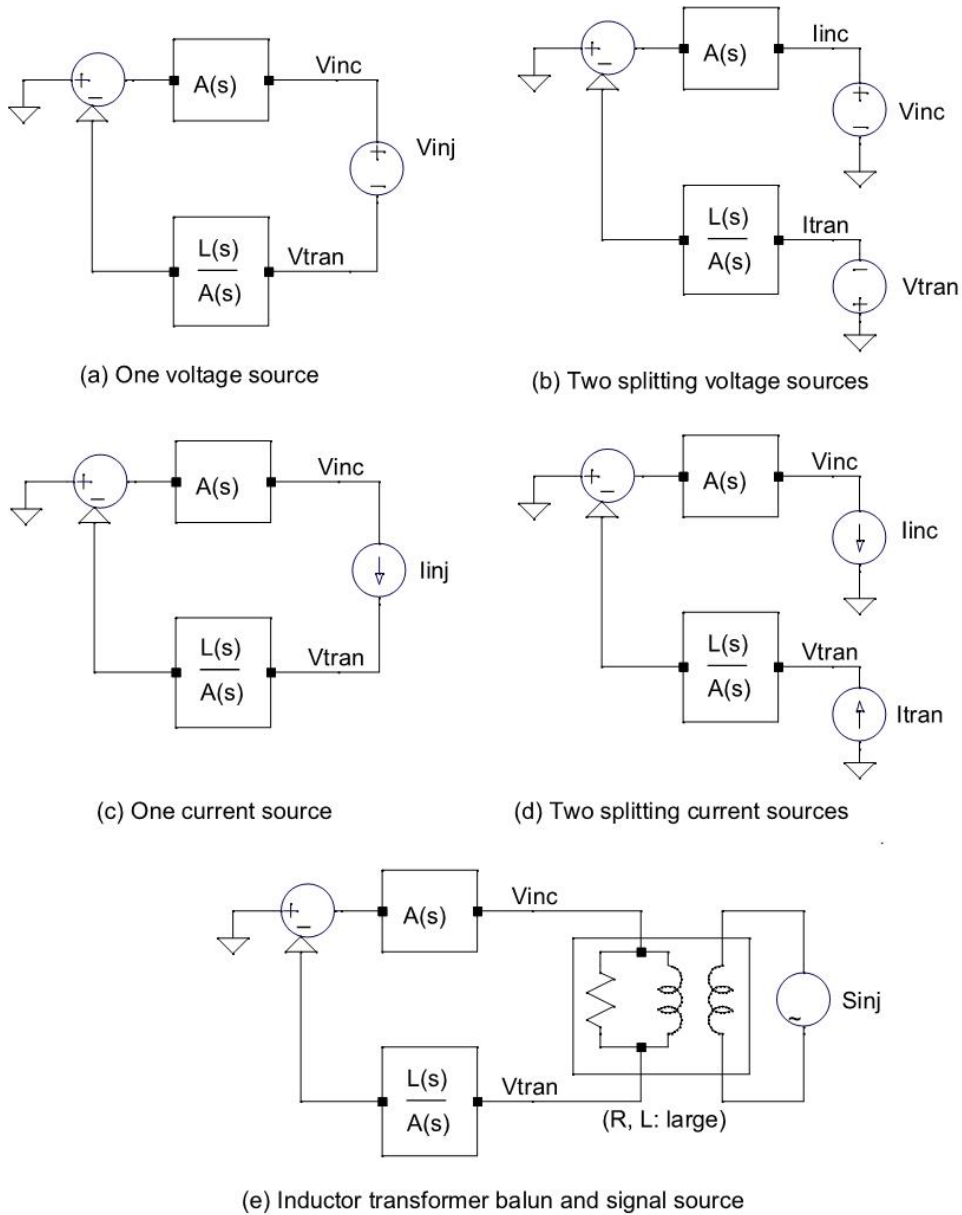


Fig. 3. Derivation of self-loop function based on alternating current conservation.

2.5. Switching regulator

In this section, a PWM waveform is presented as a superposition of many harmonic signals. A switching regulator maintains an essentially constant output voltage with changing input voltage. In

other words, the energy is converted from the input source into the average output energy in a unit of time. An increase in the duty cycle increases the output voltage, whereas a decrease in the duty cycle decreases the output voltage as shown in Fig. (4)(a). Based on the Fourier series expansion of the square wave, the waveforms of the pulse wave are expressed in many functions of time with many different frequencies as shown in Fig. (4)(b), and (4)(c). The waveforms of PWM are also expressed in many functions of time with many different frequencies which are constituted by the times of a fundamental frequency (or a unit cycle $T = t_{on} + t_{off}$). The average voltage at the output of the power conversion is defined as

$$\overline{V_{out}} = V_{in} \left(\frac{T_{on}}{T_{on} + T_{off}} \right) \tag{7}$$

The main control element of this system is a switch which controls the output voltage by rapidly switching the input voltage on and off with a duty cycle that depends on the load. The switching control source is constantly driven back and forth between saturation and cutoff.

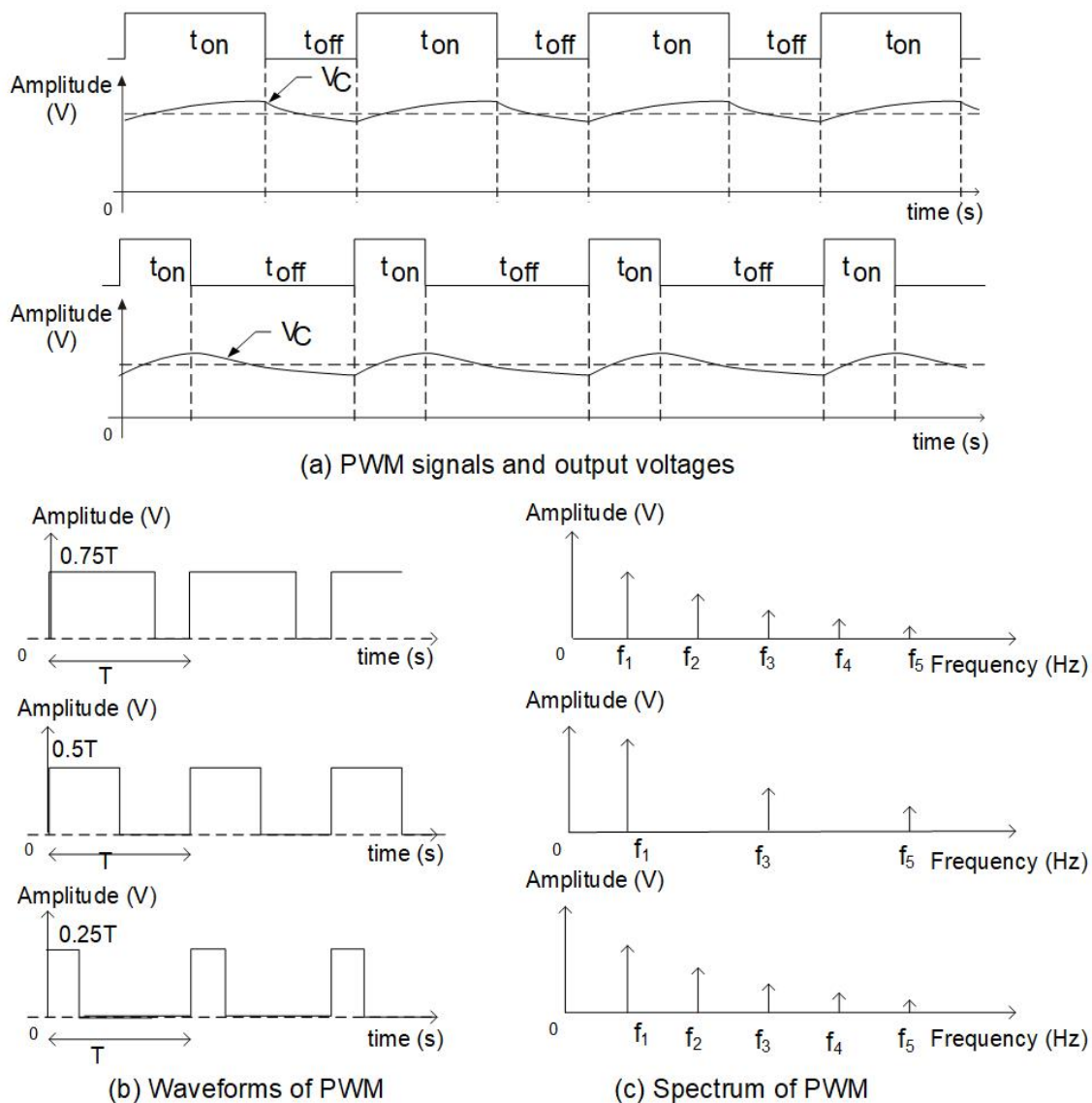


Fig. 4. Switching sources and output voltages.

Some waveform functions of the control sources are expressed in Eq. (8), Eq. (9), and Eq. (10).

$$S_{25\%PWM}(t) = \frac{4}{\pi} \sum_{k=1}^{\infty} \frac{\sin(2\pi(2k-1)(f_1)t)}{2k-1} - \frac{2}{\pi} \sum_{k=1}^{\infty} \frac{\sin(2\pi(2k-1)(2f_1)t)}{2k-1} \quad (8)$$

$$S_{50\%PWM}(t) = \frac{4}{\pi} \sum_{k=1}^{\infty} \frac{\sin(2\pi(2k-1)(f_1)t)}{2k-1} \quad (9)$$

$$S_{75\%PWM}(t) = \frac{4}{\pi} \sum_{k=1}^{\infty} \frac{\sin(2\pi(2k-1)(f_1)t)}{2k-1} + \frac{2}{\pi} \sum_{k=1}^{\infty} \frac{\sin(2\pi(2k-1)(2f_1)t)}{2k-1} \quad (10)$$

3. Analysis of second-order denominator complex function

3.1. Second-order denominator complex function

In this section, we shall analyze the frequency response of a typical second-order denominator complex function. This complex function is defined as in Eq. (11). Assume that all of the constant variables are not equal to zero. If the constant is smaller than zero, it is expressed as a complex number ($a < 0 \Rightarrow a = |a|j^2 = |a|e^{\pm j\pi}$). In this paper, the angular of the constant is not written in details.

$$H(s) = \frac{1}{as^2 + bs + c} \quad (11)$$

From Eq. (31) in Appendix A.1, the simplified complex function is written as in Eq. (12).

$$H(j\omega) = \frac{\frac{4a}{b^2}}{\left(1 + j\frac{2a}{b}\omega\right)^2 + \left(\frac{2a}{b}\right)^2 \left[\frac{c}{a} - \left(\frac{b}{2a}\right)^2\right]} \quad (12)$$

In order to plot the magnitude-angular charts, the values of magnitude-angular of the complex function, which are calculated in Appendix A.1, are summarized on Table 1. In overdamped case, the magnitude of the complex function is so high from the first cut-off angular frequency

$\omega_{cut1} = \left| \frac{b}{2a} \left(1 - \frac{2a}{b} \sqrt{\frac{c}{a} - \left(\frac{b}{2a}\right)^2} \right) \right|$ to the second cut-off angular frequency $\omega_{cut2} = \left| \frac{b}{2a} \left(1 + \frac{2a}{b} \sqrt{\frac{c}{a} - \left(\frac{b}{2a}\right)^2} \right) \right|$. Therefore,

this gain will amplify the high order harmonics from ω_{cut1} to ω_{cut2} of an input signal which includes many harmonics.

3.2. Damped oscillation noise

In this section, we describe the response of a typical second-order denominator complex function to a step input or a square wave. Based on the Fourier series expansion of the PWM wave, the waveforms of the PWM wave are expressed in many functions of time with many different frequencies as shown in Fig. 4(c).

Table 1. Summary of magnitude-angular values of transfer function

Case	Underdamped	Critically damped	Overdamped
Delta (Δ)	$\frac{c}{a} < \left(\frac{b}{2a}\right)^2 \Rightarrow \Delta = b^2 - 4ac > 0$	$\frac{c}{a} = \left(\frac{b}{2a}\right)^2 \Rightarrow \Delta = b^2 - 4ac = 0$	$\frac{c}{a} > \left(\frac{b}{2a}\right)^2 \Rightarrow \Delta = b^2 - 4ac < 0$
Module $ H(\omega) $	$\frac{4a}{b^2} \sqrt{\left(\frac{4a}{b}\omega\right)^2 + \left(1 - \left(\frac{2a}{b}\omega\right)^2 - \left(\frac{2a}{b}\right)^2 \left[\frac{c}{a} - \left(\frac{b}{2a}\right)^2\right]\right)^2}$	$\frac{4a}{b^2} \sqrt{\left(\frac{4a}{b}\omega\right)^2 + \left(1 - \left(\frac{2a}{b}\omega\right)^2\right)^2}$	$\frac{4a}{b^2} \sqrt{\left(\frac{4a}{b}\omega\right)^2 + \left(1 - \left(\frac{2a}{b}\omega\right)^2 + \left(\frac{2a}{b}\right)^2 \left[\frac{c}{a} - \left(\frac{b}{2a}\right)^2\right]\right)^2}$
Angular $\angle H(\omega)$	$\arctan \left(\frac{-\frac{4a}{b}\omega}{1 - \left(\frac{2a}{b}\omega\right)^2 - \left(\frac{2a}{b}\right)^2 \left[\frac{c}{a} - \left(\frac{b}{2a}\right)^2\right]} \right)$	$\arctan \left(\frac{-\frac{4a}{b}\omega}{1 - \left(\frac{2a}{b}\omega\right)^2} \right)$	$\arctan \left(\frac{-\frac{4a}{b}\omega}{1 - \left(\frac{2a}{b}\omega\right)^2 + \left(\frac{2a}{b}\right)^2 \left[\frac{c}{a} - \left(\frac{b}{2a}\right)^2\right]} \right)$
$\omega = \frac{b}{2a}$	$ H(\omega) < \frac{14a}{2b^2}$ $\angle H(\omega) > -\frac{\pi}{2}$	$ H(\omega) = \frac{14a}{2b^2}$ $\angle H(\omega) = -\frac{\pi}{2}$	$ H(\omega) > \frac{14a}{2b^2}$ $\angle H(\omega) < -\frac{\pi}{2}$

- In under-damped case, the high-order harmonics of the step signal are significantly reduced from the first cut-off angular frequency. Therefore, the rising time and falling time are rather short. In this case, the system is absolutely stable.
- In case of critically damped, the rising time and falling time are longer than the underdamped case. Now, the system is marginally stable. The energy propagation is also maximal because this condition is equal to the balanced charge-discharge time condition [9].
- In over-damped case of the complex function, the gain at the cut-off angular frequency will amplify the high-order harmonics of the step signal that causes the peaking or ringing. Ringing is an unwanted oscillation of a voltage or current. The term of “damped oscillation noise” is proposed to define this unwanted oscillation which fades away with time, particularly in the step response (the response to a sudden change in input). Damped oscillation noise is undesirable because it causes extra current to flow, which leads to thereby wasting energy and causing extra heating of the components. It can cause unwanted electromagnetic radiation to be emitted. Therefore, the system is unstable.

3.3. Self-loop function of second-order denominator complex function

In this section, we investigate the characteristics of the self-loop function $L(s)$ on the magnitude-angular plots and the polar chart. The general transfer function and self-loop function are rewritten as in Eq. (13). The magnitude-angular values and the real-imaginary values of the self-loop function, which are calculated in Appendix A.2, are summarized in Table 2. In this work, the self-loop function is sketched on the magnitude-angular charts and polar plots.

$$H(j\omega) = \frac{\frac{4a}{b^2}}{1 + \left(\frac{2a}{b}\right)^2 (j\omega)^2 + 2\left(\frac{2a}{b}\right)j\omega + \left(\frac{2a}{b}\right)^2 \left[\frac{c}{a} - \left(\frac{b}{2a}\right)^2\right]}; L(j\omega) = j\frac{4a}{b}\omega - \left(\frac{2a}{b}\omega\right)^2 + \left(\frac{2a}{b}\right)^2 \left[\frac{c}{a} - \left(\frac{b}{2a}\right)^2\right] \quad (13)$$

4. Analysis of power stage of step-down switching buck converter

4.1. Time domain analysis of power stage

In this section, the time domain refers to the analysis of the power stage of a buck converter with respect to time. In the time domain, the behavior of a system can be described by a differential equation. Therefore, the differential equation plays a prominent role in engineering.

Table2. Summary of magnitude-angular values and real-imaginary values of self-loop function

Case	Underdamped		Critically damped		Overdamped	
Delta (Δ)	$\Delta = b^2 - 4ac > 0$		$\Delta = b^2 - 4ac = 0$		$\Delta = b^2 - 4ac < 0$	
$ L(j\omega) $	$\sqrt{\left(\frac{4a}{b}\omega\right)^2 + \left[\left(\frac{2a}{b}\right)^2 \left[\frac{c}{a} - \left(\frac{b}{2a}\right)^2\right] - \left(\frac{2a}{b}\omega\right)^2\right]^2}$		$\sqrt{\left(\frac{4a}{b}\omega\right)^2 + \left(\frac{2a}{b}\omega\right)^4}$		$\sqrt{\left(\frac{4a}{b}\omega\right)^2 + \left[-\left(\frac{2a}{b}\right)^2 \left[\frac{c}{a} - \left(\frac{b}{2a}\right)^2\right] - \left(\frac{2a}{b}\omega\right)^2\right]^2}$	
$\angle L(j\omega)$	$\arctan\left(\frac{\frac{4a}{b}\omega}{\left[\left(\frac{2a}{b}\right)^2 \left[\frac{c}{a} - \left(\frac{b}{2a}\right)^2\right] - \left(\frac{2a}{b}\omega\right)^2\right]}\right)$		$\arctan\left(\frac{2}{\left(\frac{2a}{b}\omega\right)}\right)$		$\arctan\left(\frac{\frac{4a}{b}\omega}{-\left[\left(\frac{2a}{b}\right)^2 \left[\frac{c}{a} - \left(\frac{b}{2a}\right)^2\right] - \left(\frac{2a}{b}\omega\right)^2\right]}\right)$	
$\omega = \frac{b}{2a}\sqrt{\sqrt{5}-2}$	$ L(\omega) > 1$	$\angle L(\omega) < -76.3^\circ$	$ L(\omega) = 1$	$\angle L(\omega) = -76.3^\circ$	$ L(\omega) < 1$	$\angle L(\omega) > -76.3^\circ$
$\omega = \frac{b}{2a}$	$ L(\omega) > \sqrt{5}$	$\angle L(\omega) < -63.4^\circ$	$ L(\omega) = \sqrt{5}$	$\angle L(\omega) = -63.4^\circ$	$ L(\omega) < \sqrt{5}$	$\angle L(\omega) > -63.4^\circ$
$\omega = \frac{b}{a}$	$ L(\omega) > 4\sqrt{2}$	$\angle L(\omega) < -45^\circ$	$ L(\omega) = 4\sqrt{2}$	$\angle L(\omega) = -45^\circ$	$ L(\omega) < 4\sqrt{2}$	$\angle L(\omega) > -45^\circ$
$\text{Re}\{L(j\omega)\}$	$-\left(\frac{2a}{b}\omega\right)^2 + \left[\left(\frac{2a}{b}\right)^2 \left[\frac{c}{a} - \left(\frac{b}{2a}\right)^2\right] - \left(\frac{2a}{b}\omega\right)^2\right]$		$-\left(\frac{2a}{b}\omega\right)^2$		$-\left(\frac{2a}{b}\omega\right)^2 - \left[\left(\frac{2a}{b}\right)^2 \left[\frac{c}{a} - \left(\frac{b}{2a}\right)^2\right] - \left(\frac{2a}{b}\omega\right)^2\right]$	
$\text{Im}\{L(j\omega)\}$	$\frac{4a}{b}\omega$		$\frac{4a}{b}\omega$		$\frac{4a}{b}\omega$	
$\omega = \frac{b}{2a}\sqrt{\sqrt{5}-2}$	$\text{Re} < 2 - \sqrt{5}$	$\text{Im} = 2\sqrt{\sqrt{5}-2}$	$\text{Re} = 2 - \sqrt{5}$	$\text{Im} = 2\sqrt{\sqrt{5}-2}$	$\text{Re} > 2 - \sqrt{5}$	$\text{Im} = 2\sqrt{\sqrt{5}-2}$
$\omega = \frac{b}{2a}$	$\text{Re} < -1$	$\text{Im} = 2$	$\text{Re} = -1$	$\text{Im} = 2$	$\text{Re} > -1$	$\text{Im} = 2$
$\omega = \frac{b}{a}$	$\text{Re} < -4$	$\text{Im} = 4$	$\text{Re} = -4$	$\text{Im} = 4$	$\text{Re} > -4$	$\text{Im} = 4$

A solution of a differential equation is a set of functions that satisfy the equation. Only the simplest differential equation is solvable by explicit formulas; however, many properties of the solution of a given differential equation may be determined without computing them exactly. Consider a parallel RLC circuit with a DC voltage source, a switch, a diode, an inductor, a capacitor, and a resistor in Fig.

5. Here, the cut-off and the resonant angular frequency are defined as $\omega_{2RC} = \frac{1}{2RC}$; $\omega_{LC} = \frac{1}{\sqrt{LC}}$.

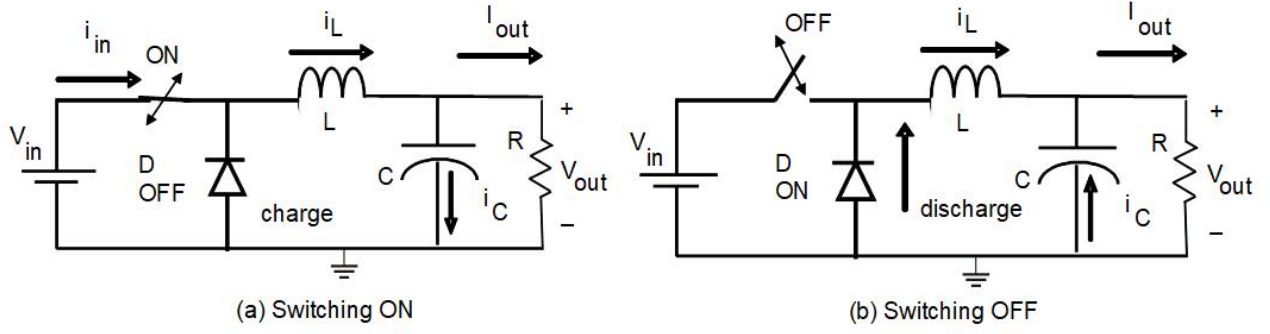


Fig. 5. RLC network in power stage of switching power converter.

As switch is ON, from Appendix A.3, Eq. (69) the differential equation is

$$\frac{d^2 V_{out}(t)}{dt^2} + \frac{1}{RC} \frac{dV_{out}(t)}{dt} + \frac{V_{out}(t)}{LC} = 0 \quad (14)$$

And, from Appendix A.3, Eq. (73) the output voltage is

$$V_{charge}(t) = A_{ch1} e^{\left(-\omega_{2RC} + \sqrt{(\omega_{2RC})^2 - \omega_{LC}^2}\right)t} + A_{ch2} e^{\left(-\omega_{2RC} - \sqrt{(\omega_{2RC})^2 - \omega_{LC}^2}\right)t} \quad (15)$$

As switch is OFF, from Appendix A.3, Eq. (79) the differential equation is

$$\frac{d^2 V_{dis}(t)}{dt^2} - \frac{1}{RC} \frac{dV_{dis}(t)}{dt} + \frac{V_{dis}(t)}{LC} = 0 \quad (16)$$

And, from Appendix A.3, Eq. (83), the output voltage is

$$V_{discharge}(t) = A_{dis1} e^{\left(\omega_{2RC} + \sqrt{(\omega_{2RC})^2 - \omega_{LC}^2}\right)t} + A_{dis2} e^{\left(\omega_{2RC} - \sqrt{(\omega_{2RC})^2 - \omega_{LC}^2}\right)t} \quad (17)$$

From Eq. (7), Eq. (15) and Eq. (17), in one cycle of the switching time, the average voltage of the capacitor is expressed as

$$\overline{V_{out}} = \frac{1}{(T_{ON} + T_{OFF})} \left(\int_0^{T_{ON}} \left(A_{ch1} e^{\left(-\omega_{2RC} + \sqrt{(\omega_{2RC})^2 - \omega_{LC}^2}\right)t} + A_{ch2} e^{\left(-\omega_{2RC} - \sqrt{(\omega_{2RC})^2 - \omega_{LC}^2}\right)t} \right) dt + \int_{T_{ON}}^{T_{ON} + T_{OFF}} \left(A_{dis1} e^{\left(\omega_{2RC} + \sqrt{(\omega_{2RC})^2 - \omega_{LC}^2}\right)t} + A_{dis2} e^{\left(\omega_{2RC} - \sqrt{(\omega_{2RC})^2 - \omega_{LC}^2}\right)t} \right) dt \right) \quad (18)$$

To generate a stable output voltage without overshoot, the balanced charge-discharge time condition is defined by

$$\omega_{2RC} = \omega_{LC} \Leftrightarrow \omega = \frac{1}{\sqrt{LC}} = \frac{1}{2RC} \quad (19)$$

4.2. Frequency domain analysis of power stage

In this section, we shall present the frequency response of a power stage of a buck converter. The response of a system, as a function of frequency, is described by a complex function. One of the main reasons for using a frequency domain representation of a problem is to simplify the mathematical analysis. It is easier to solve a linear differential equation by converting the description of the system from the time domain to a frequency domain. The qualitative behavior of the system can be easily understood such as bandwidth, frequency response, gain, harmonics, spectrum... Moreover, any sources can be expressed as a wave function in analog signal processing. Based on the switching frequency of the control signal, the input supply source is transferred from a DC supply source into an AC supply signal which contains a lot of harmonics. Models of circuit and measurement of self-loop function for the power stage are shown in Fig. 6.

The transfer function and the self-loop function of this network, which are calculated in Appendix A.4., are simplified as

$$H(s) = \frac{1}{LCs^2 + s\frac{L}{R} + 1}; L(s) = LCs^2 + s\frac{L}{R} \quad (20)$$

Then, the denominator is modified as

$$H(s) = \frac{\frac{4R^2C}{L}}{(2RCs + 1)^2 + (2RC)^2 \left[\frac{1}{LC} - \left(\frac{1}{2RC} \right)^2 \right]} \quad (21)$$

To transfer the maximum power, the denominator of Eq. (21) has to be maximal. So, the constrained condition is

$$\frac{1}{LC} - \left(\frac{1}{2RC} \right)^2 = 0 \Rightarrow \omega = \frac{1}{\sqrt{LC}} = \frac{1}{2RC} \quad (22)$$

The constraints for the stability are defined as

$$\frac{1}{LC} > \left(\frac{1}{2RC} \right)^2 \Rightarrow |Z_L| = |Z_C| < 2R \rightarrow \text{Instability} \quad (23)$$

$$\frac{1}{LC} = \left(\frac{1}{2RC} \right)^2 \Rightarrow |Z_L| = |Z_C| = 2R \rightarrow \text{Marginal stability} \quad (24)$$

$$\frac{1}{LC} < \left(\frac{1}{2RC} \right)^2 \Rightarrow |Z_L| = |Z_C| > 2R \rightarrow \text{Stability} \quad (25)$$

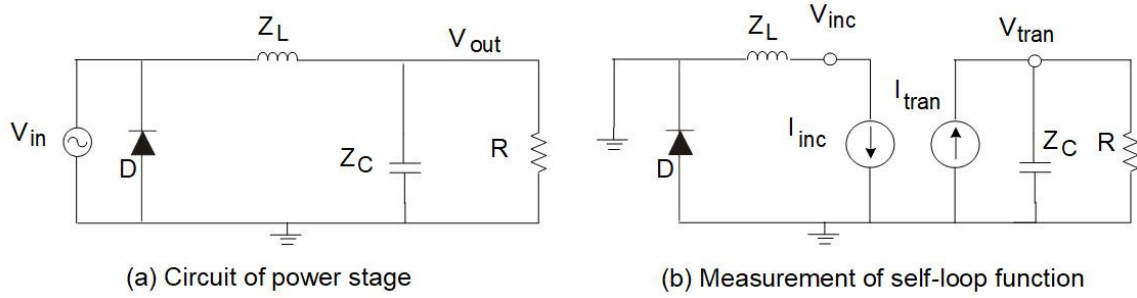


Fig. 6. Models of circuit and measurement of self-loop function for power stage.

4.3. Stability test for power stage of buck converter

This section will present a stability test for a power stage of a buck converter. Three models of the power stage are used to do the damped oscillation noise test. The marginally stable model is designed at cut-off frequency $f_0 = 500$ kHz taking $L = 0.796$ μ H, $C = 31.8$ nF, and $R = 2.5$ Ω based on a balanced charge and discharge time condition as shown in Fig. 7(b). Figs. 7(a) and 7(c) are unconditionally stable ($R = 1$ Ω), and unstable ($R = 5$ Ω), respectively. Figs. 7(d), 7(e) and 7(f) are the measurements of the self-loop functions. Fig. 8(a) represents the SPICE simulation results of the magnitude and phase of the power stage circuit on the frequency domain. In time domain, when the pulse signals go in to these models, the transient responses are shown in Fig. 8(b). The damped oscillation noise (red) occurs in case of the unstable network. The measurements of the self-loop functions of the proposed models on the polar chart and the magnitude-angular plots are shown in Figs. 8(c),(d). In theoretical calculation at the cut-off frequency 500 kHz is -76.3 degrees. Our simulation results of self-loop function show that

- In stable case, phase is 95.7 degrees at 500 kHz, (phase margin = -84.3 degrees).
- In marginally stable case, phase is 104 degrees at 500 kHz, (phase margin = -76 degrees).
- In unstable case, phase margin is 116 degrees at 500 kHz, (phase margin = -64 degrees).

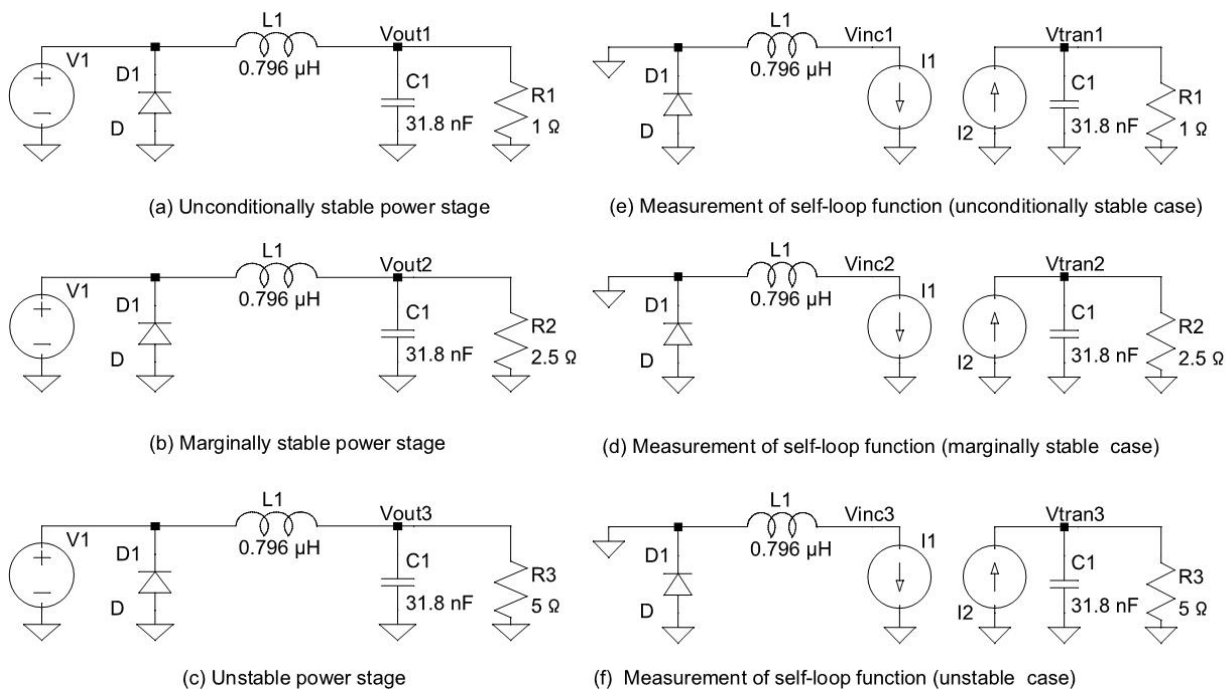


Fig. 7. Models of circuits and measurements of self-loop functions for power stage.

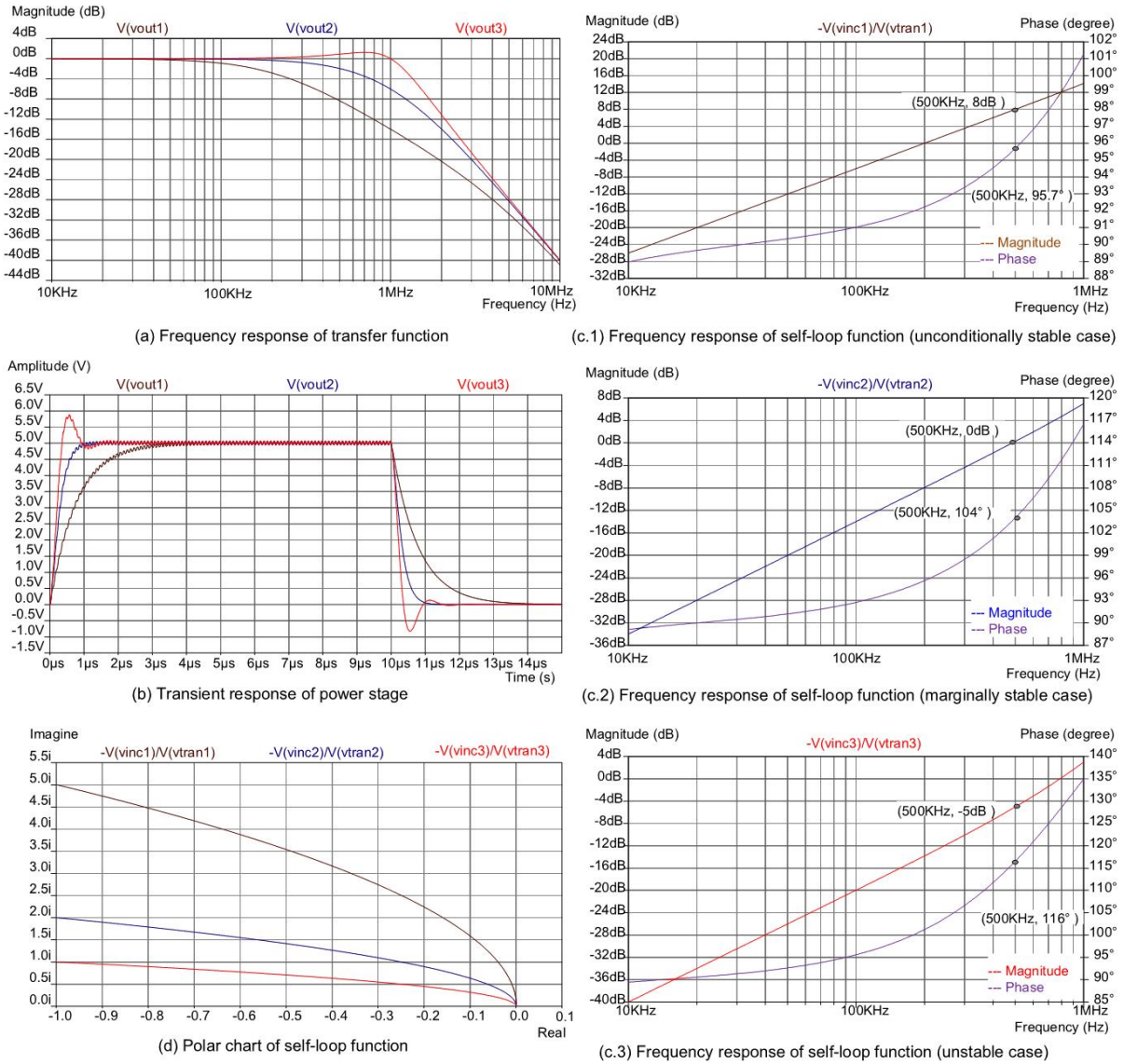


Fig. 8. Frequency response of transfer function, transient response with pulse input, polar chart and magnitude-phase plots of self-loop function for power stage.

On the polar plots of self-loop functions, the stability tests of these models are shown in Fig. 10(c). The characteristics of a self-loop function are divided into three regions: (brown) unconditionally stable, (blue) marginally stable, and (red) unstable. The simulation results and the values of theoretical calculation are unique. The constraints for passive components (R, L, and C) are

- Unconditionally stable ($|Z_L|=|Z_C|>2R$), phase margin is smaller than -76.3 degrees at unity gain.
- Marginally stable ($|Z_L|=|Z_C|=2R$), the phase margin is -76.3 degrees at unity gain.
- Unstable ($|Z_L|=|Z_C|<2R$), the phase margin is greater than -76.3 degrees at unity gain.

4.4. Overshoot improvement with RLC network

This section presents an overshoot improvement technique using a parallel RLC network. In case that the values of R, L, and C do not satisfy the balanced charge-discharge time condition ($|Z_L|=|Z_C|<2R$), the overshoot voltages are improved by a parallel RLC circuit as shown in Fig. 9.

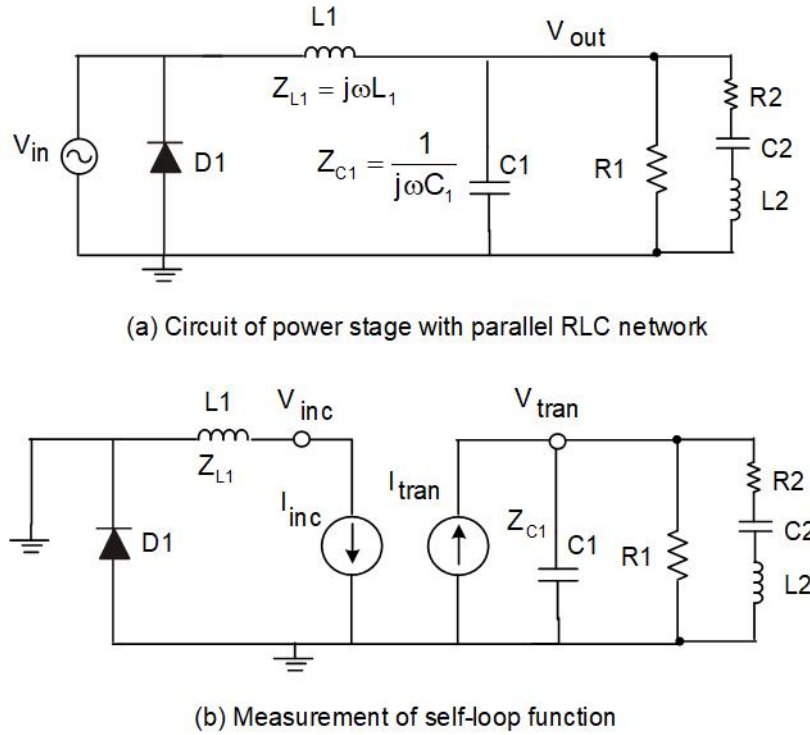


Fig. 9. Power stage of switching power conversion system with parallel RLC network.

The transfer function and the self-loop function of this network, which are calculated in Appendix A.5., are simplified as

$$H(j\omega) = \frac{1}{1 + j\omega \frac{L_1}{R_1} - \omega^2 \left(L_1 C_1 + \frac{C_2 L_1}{1 - L_2 C_2 \omega^2 + j\omega C_2 R_2} \right)}; L(s) = j\omega \frac{L_1}{R_1} - \omega^2 \left(L_1 C_1 + \frac{C_2 L_1}{1 - L_2 C_2 \omega^2 + j\omega C_2 R_2} \right) \quad (26)$$

When the overshoot improvement is considered, the transfer function of the power stage of the buck converter is a fourth-order denominator complex function. It is very difficult to investigate the stable regions of this complex function. So, the measurement of the self-loop function is very important to do the stability test for the buck converter.

4.5. SPICE simulation results of overshoot improvement

This section is focused on the overshoot improvement with a parallel RLC network. In case the balanced charge - discharge time condition is not satisfied, the overshoot is a big problem. The parallel RLC is designed at cut-off frequency $f_0 = 500$ kHz taking $L_2 = 4.55$ uH, $C_2 = 11.4$ nF, and $R_2 = 20$ Ω . The frequency responses and the measurement of self-loop function are shown in Fig. 10. On time domain, when the parallel RLC network is added, the damped oscillation noise is reduced from 0.8 V to 0.1 V as shown in Fig. 11. The phase margin is improved from -64 degrees to -62 degrees at the cut-off frequency $f_0 = 500$ kHz. Our simulation results of self-loop function show that

- In marginally stable case, phase is 104 degrees at 500 kHz, (phase margin = -76 degrees).
- In unstable case, phase margin is 116 degrees at 500 kHz, (phase margin = -64 degrees).
- Overshoot improvement with parallel RLC, phase margin is 118 degrees at 500 kHz, (phase margin = -62 degrees).

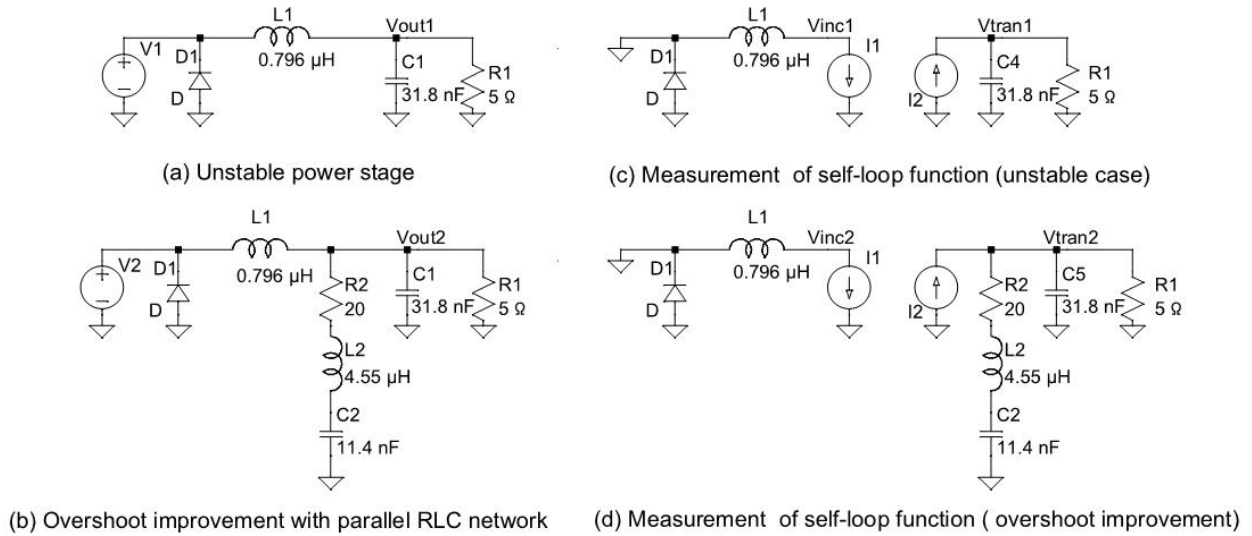


Fig. 10. Overshoot improvement of switching buck converter with parallel RLC network.

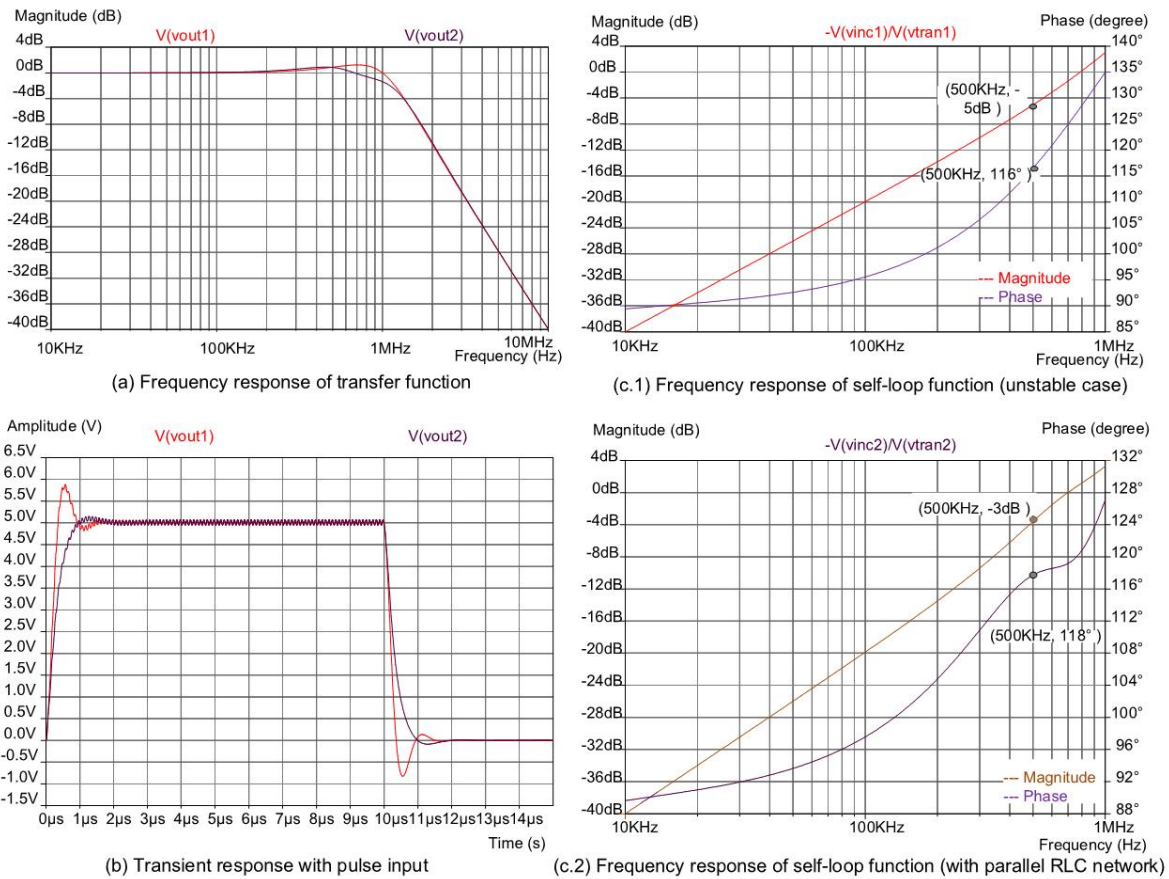


Fig. 11. Frequency response of transfer function, transient response with pulse input, and magnitude-phase plots of self-loop function for power stage with parallel RLC network.

4.6. Adaptive feedback loop

This section analyzes the adaptive feedback loop of the buck converter. An adaptive feedback loop is required for some switching power supplies because some parameters of the desired processing operation are changing. The closed loop adaptive network uses feedback in the form of an error signal

to refine its transfer function. Switching power supplies rely on negative feedback to maintain the output voltages at their specified value. To accomplish this, a differential amplifier is used to sense the difference between a reference voltage and the actual output voltage to establish a small error signal (V_{cont}). A feedback loop of the output voltage is used to keep stable average output as shown in Fig. 12. It follows from Eq. (28) that the control voltage is dependent on the loop filter of the local feedback of the op-amp. From Appendix A.6, Eq. (89), the control voltage is expressed as

$$V_{cont} = V_{ref} + \frac{(1 + j\omega R_1 C_1)(1 + j\omega R_2 C_2)}{j\omega R_1 C_2} (V_{ref} - V_{out}) \quad (27)$$

The magnitude of the control voltage is rewritten as

$$|V_{cont}| = V_{ref} + \frac{\sqrt{(\omega^2 R_1 C_1 R_2 C_2 - 1)^2 + \omega^2 (R_1 C_1 + R_2 C_2)^2}}{\omega R_1 C_2} (V_{ref} - V_{out}) \quad (28)$$

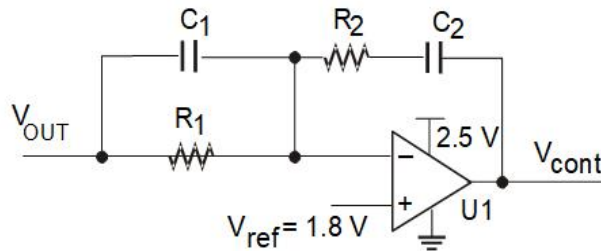


Fig. 12. Adaptive feedback loop.

4.7 Ripple improvement with spread spectrum technique

This section describes a ripple improvement based on the spread spectrum of the PWM signal. A PWM signal can be expressed by a function of time which includes many different frequencies. The spectrum of PWM is constituted of the times of a fundamental frequency. The ripple noise is located at these frequencies. Therefore, a fundamental harmonic notch filter [5] is proposed to reduce the noise of the fundamental harmonic as shown in Fig. 13. The frequency modulation is taken place at the variable controlled oscillator (VCO). The time duty on and off in one cycle (T_{ON} , T_{OFF}) of the control signals are divided into many shorter duties. Therefore, the energy of the input source is spread in the frequency domain; or the ripple is kept smaller as shown in Fig. 13. Here, K : sensitivity of VCO ($\omega_{VCO} = KV_b$); V_b : bias voltage; V_m : modulation signal

$$V_m(t) = A_m \cos(2\pi f_m t) = A_m \left(1 - \frac{(2\pi f_m t)^2}{2!} + \frac{(2\pi f_m t)^4}{4!} - \frac{(2\pi f_m t)^6}{6!} + \dots \right) \quad (29)$$

Here, $\phi_m(t) = KA_m \cos(2\pi f_m t)$; $S_{VCO}(t) = A_{VCO} \cos[\omega_{VCO} t + \phi_m(t)]$, the function of the frequency modulation signal is

$$S_{VCO}(t) = A_{VCO} \cos \left[KV_b t + KA_m \left(1 - \frac{(2\pi f_m t)^2}{2!} + \frac{(2\pi f_m t)^4}{4!} - \frac{(2\pi f_m t)^6}{6!} + \dots \right) \right] \quad (30)$$

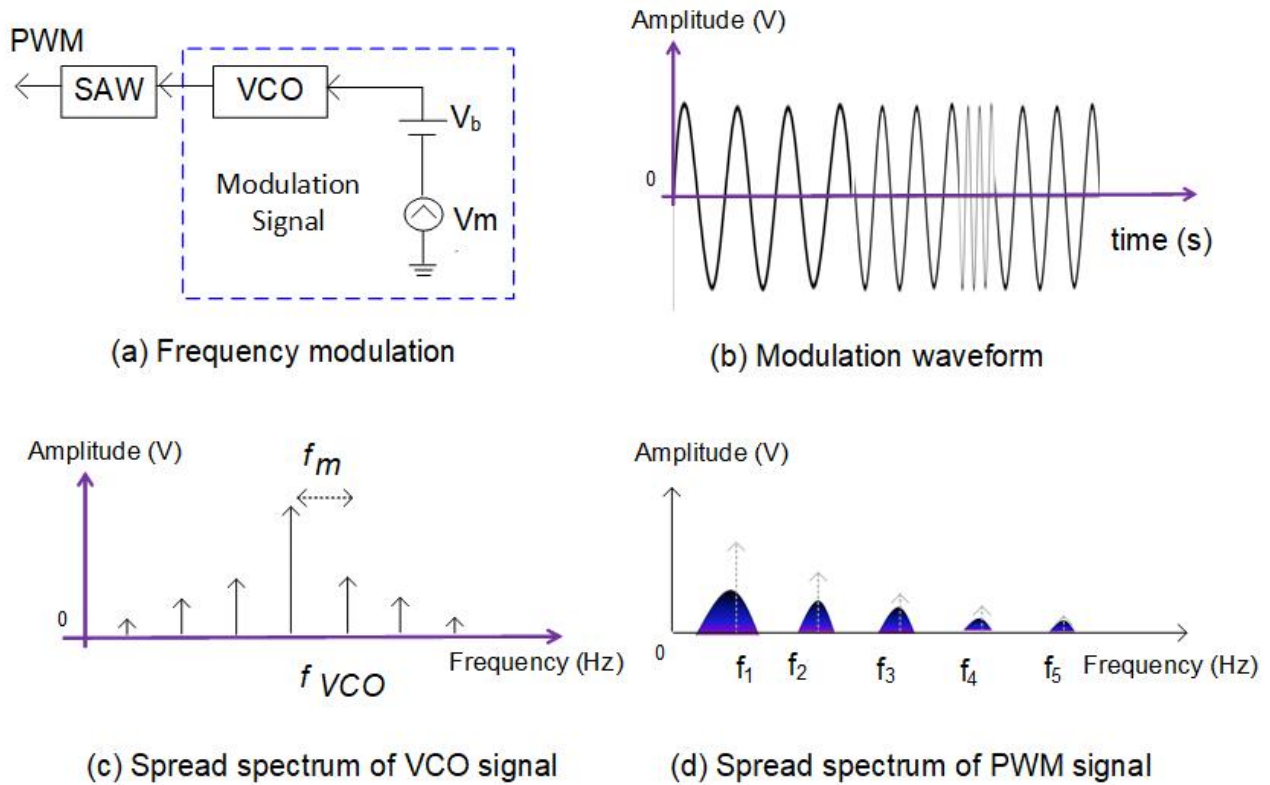


Fig.13. Ripple reduction based on spread spectrum of PWM signal.

5. Proposed design of step-down switching power converter

5.1. Design of step-down switching power converter

This section presents the proposed design of the buck converter. Fig. 14 shows a block diagram of an inductor type buck converter. The operation parameters of this design are described in Table 3. A supply voltage of 12V was applied to the converter and the output voltage was set to 5V. The system consists of two loops: the main loop goes from the output of buck converter to the input of the controller, and the secondary loop is the adaptive feedback.

Table 3: Operation parameters of step-down switching power conversion.

Input Voltage (V_{in})	12 V
Output Voltage (V_o)	5.0 V
Output Current (I_o)	0.5 A
Clock Frequency (F_{ck})	2 MHz
Current Step (ΔI_o)	1 A
Output Ripple	0.05 mVpp
Over-shoot	0.1 mV
Under-shoot	0.1 mV

The switching frequency was set at 2MHz. In this system, the cutoff frequency is designed at $f_{cut} = \frac{1}{2\pi\sqrt{LC}} = \frac{1}{4\pi RC} = 500\text{ kHz}$ ($R = 5\ \Omega$, $L = 0.796\ \mu\text{H}$, $C = 31.8\ \text{nF}$). The parallel RLC is designed at cut-off frequency $f_0 = 500\ \text{kHz}$ taking $L_P = 4.55\ \mu\text{H}$, $C_P = 11.4\ \text{nF}$, and $R_P = 20\ \Omega$. This converter consists of a monolithic controller and several external passive components. The large inductors and capacitors are used as off-chip components. Apart from those passive components, other circuit blocks can be implemented on-chip.

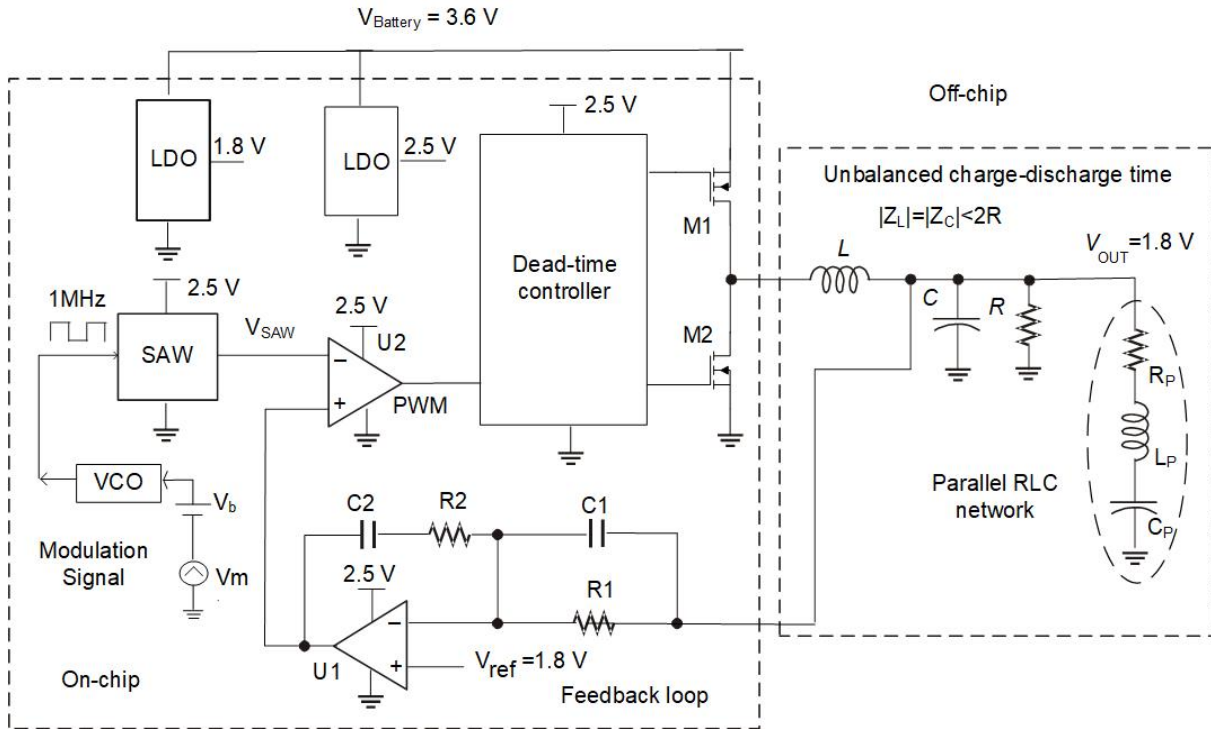


Fig.14. Step-down switching power conversion with parallel RLC network.

5.2 SPICE simulation results of proposed design

This section describes the SPICE simulation results for the proposed design of the buck converter. On this model as being described in Fig. 14, the spectrums of the control signals are spread. The ripples of the output energy are reduced (smaller than 0.05 mV) by a modulated control signal as shown in Fig. 15. The spectrums of the switching noise are kept less than 10 micro-volts compared to the set voltage of 5 V. The transient time response of the set voltage is fast 0.2 ms. On time domain, when the parallel RLC network is added, the damped oscillation noise is reduced from 0.8 V to 0.2 V.

6. Discussion

This research grew out of a set of conference papers. The paper attempts to provide an understanding or the salient features of network analysis, beginning with the mathematics describing an actual circuit model and continuing with the introduction of the complex function and the stability test of filters. The mathematical description of various transfer function employs the angular frequency variable. Given a transfer function, the self-loop function is established. Then, the frequency response of the self-loop function is obtained, into which the stability test is subsequently introduced. The self-loop function of a system is only important if it gives some useful information about relative stability or if it helps

optimize the transfer function. The self-loop function can be directly calculated based on the widened superposition principle.

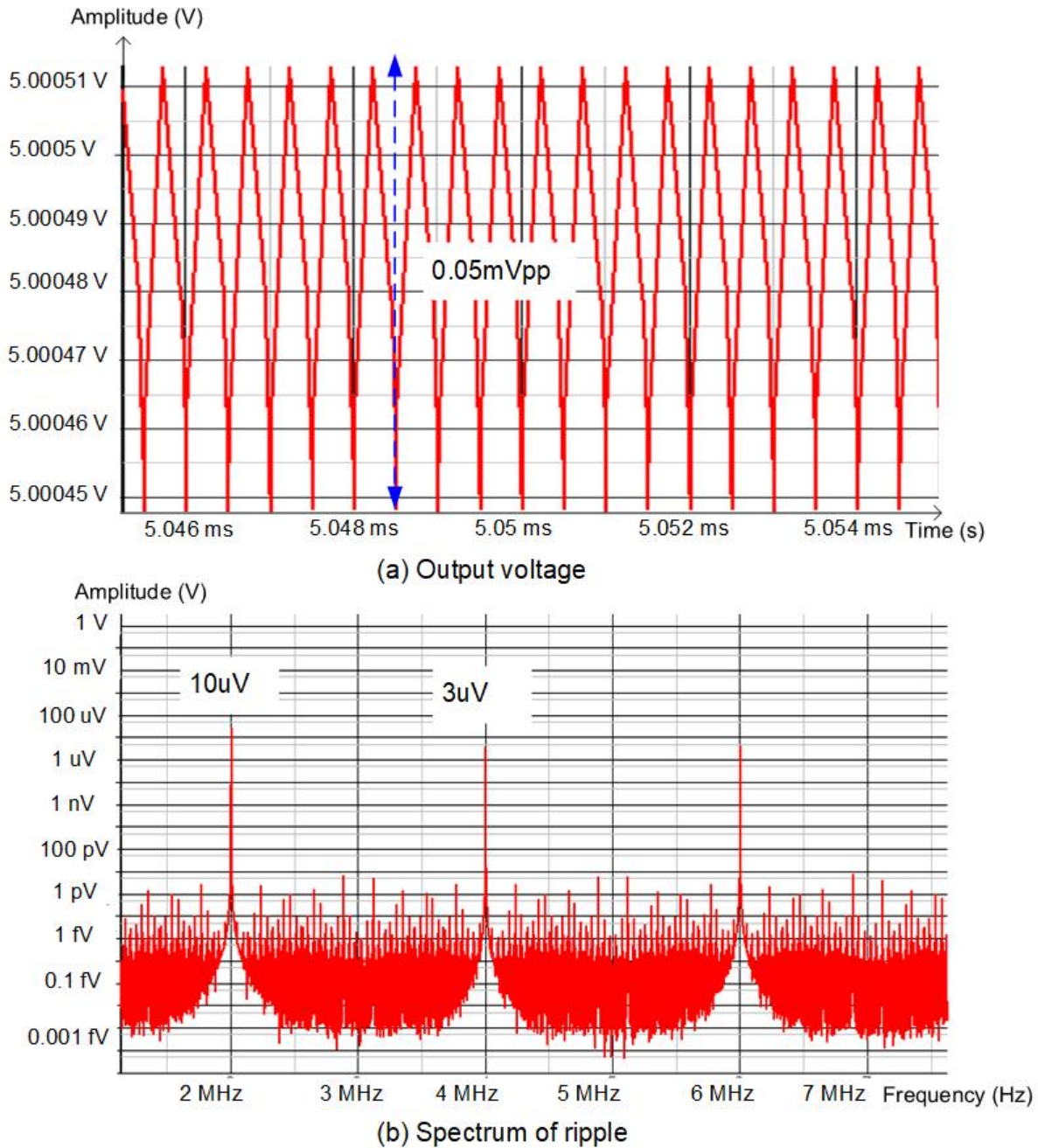


Fig.15. Simulation results of output voltage and spectrum of ripple.

The alternating current conservation technique (voltage injection) can measure the self-loop function of low-pass filters. Compared to the research results with mathematical analysis, the properties of self-loop functions are the same. SPICE simulation results are included. Moreover, Nyquist theorem shows that the polar plot of self-loop function $L(s)$ must not encircle the point $(-1, 0)$ clockwise as s traverses a contour around the critical region clockwise in polar chart [10,11]. However, Nyquist theorem is only used in theoretical analysis for feedback systems. Therefore, the stable condition of a self-loop function is a more efficient way of analyzing the method than Nyquist criterion, because it is fairly straightforward and also more powerful from an analyzing point of view.

7. Conclusion

This paper describes the approach to do the stability test for a step-down buck converter. The transfer function of the power stage of this converter is a second-order denominator complex function. Moreover, the term of “self-loop function” is proposed to define $L(s)$ in a general transfer function. In order to show an example of how to define the operating region of a second-order passive filter, a second-order denominator complex function is analyzed. In overdamped case, the filter will amplify the high order harmonics from the first cut-off angular frequency ω_{cut1} to the second cut-off angular frequency ω_{cut2} of a step input. This causes the unwanted noise which is called ringing or overshoot.

The term of “damped oscillation noise” is proposed to define the ringing. The values of the passive components used in the filter circuit were chosen directly by the stable conditions. All of the transfer functions were derived based on the widened superposition principle and self-loop functions were measured according to the alternating current conservation technique.

A new architecture is proposed to overcome the limitation of the conventional architecture and to improve the efficiency of the converter. The obtained results were acquired to simulations using SPICE models of the devices. The overshoot is canceled based on a balanced charge-discharge time condition $T = 2\pi\sqrt{LC} = 4\pi RC$ when R, L and C components are chosen by a relation $|Z_L| = |Z_C| = 2R$. The EMI noise is reduced by a fundamental notch harmonic filter. This research is designed in TSMC 0.18 μ m CMOS technology and simulation results are provided to validate the methodology. The characteristics of the output voltage of this system are fast response, small stable ripple (smaller than 0.05 mV peak-to-peak), and low EMI noises (below 10 micro-volts compared to the set voltage of 5 V). The parallel RLC network reduced the damped oscillation noise from 0.8 V to 0.2 V. The phase margin is kept smaller (from -64 degrees to -62 degrees at the cut-off frequency $f_0 = 500$ kHz). Therefore, this model is suitable in many low energy propagation applications.

In this paper not only the results of the mathematical model but also the results of simulation of the designed circuits are provided, including the stability test. The simulation results and the values of theoretical calculation of the self-loop function are unique. Furthermore, managing power consumption of circuits and systems is one of the most important challenges for the semiconductor industry [12,13]. Therefore, the damped oscillation noise test can be used to evaluate the stability of a buck converter. There are many limitations in this system when its input sources are ideal DC signal and the PWM signals are not changed by a switch. In future work, the input signals and parasitic of the RLC and other components in these systems will be analyzed and modeled.

References

- [1] H. Kobayashi, T. Nabeshima, “Handbook of Power Management Circuits”, *Pan Stanford Publishers*, 2016.
- [2] M. Tran, N. Miki, Y. Sun, Y. Kobori, H. Kobayashi, "EMI Reduction and Output Ripple Improvement of Switching DC-DC Converters with Linear Swept Frequency Modulation", *IEEE 14th International Conference on Solid-State and Integrated Circuit Technology*, (Qingdao, China) Nov. 2018.
- [3] M. Tran, N. Miki, Y. Sun, Y. Kobori, H. Kobayashi, "EMI Reduction and Output Ripple Improvement of Switching DC-DC Converters with Linear Swept Frequency Modulation", *International Conference on Advanced Micro-Device Engineering*, (Kiryu, Japan) Dec. 2018.
- [4] M. Tran, Y. Sun, N. Oiwa, Y. Kobori, A. Kuwana, H. Kobayashi, "Mathematical Analysis and Design of Parallel RLC Network in Step-down Switching Power Conversion System", *Proceedings of International Conference on Technology and Social Science*, (Kiryu, Japan) May 2019.

- [5] H. Kobayashi, M. Tran, K.Asami, A.Kuwana, H. San, "Complex Signal Processing in Analog, Mixed - Signal Circuits", *Proceedings of International Conference on Technology and Social Science*, (Kiryu, Japan), May 2019.
- [6] M. Tran, N. Kushita, A. Kuwana, H. Kobayashi, "Flat Pass-Band Method with Two RC Band-Stop Filters for 4-Stage Passive RC Quadratic Filter in Low-IF Receiver Systems", *IEEE 13th International Conference on ASIC (ASICON 2019)* (Chongqing, China) Nov. 2019.
- [7] R. Middlebrook, "Measurement of Self-Loop Function in Feedback Systems", *Int. J. Electronics*, vol 38, No. 4, pp. 485-512, 1975.
- [8] M. Tran, "Damped Oscillation Noise Test for Feedback Circuit Based on Comparison Measurement Technique", *73rd System LSI Joint Seminar, Tokyo Institute of Technology*, (Tokyo, Japan), Oct. 2019.
- [9] M. Tran, Y. Sun, Y. Kobori, A. Kuwana, H. Kobayashi "Overshoot Cancelation Based on Balanced Charge-Discharge Time Condition for Buck Converter in Mobile Applications", *IEEE 13th International Conference on ASIC (ASICON 2019)* (Chongqing, China), Nov. 2019.
- [10] R. Boylestad, L. Nashelsky, *Electronic Devices and Circuit Theory* (11th ed.), *Pearson New International Edition*, 2012.
- [11] R. Schaumann and M. Valkenberg, "Design of Analog Filters", *Oxford University Press*, 2001.
- [12] H. Kobayashi, N. Kushita, M. Tran, K. Asami, H. San, A. Kuwana "Analog - Mixed-Signal - RF Circuits for Complex Signal Processing", *IEEE 13th International Conference on ASIC (ASICON 2019)* (Chongqing, China), Nov. 2019.
- [13] J. Wang, G. Adhikari, N. Tsukiji, M. Hirano, H. Kobayashi, K. Kurihara, A. Nagahama, I. Noda, K. Yoshii, "Equivalence Between Nyquist and Routh-Hurwitz Stability Criteria for Operational Amplifier Design", *IEEE International Symposium on Intelligent Signal Processing and Communication Systems*,(Xiamen, China), Nov. 2017.

Appendix

A.1. Second-order denominator complex function

From Eq. (11), the transfer function is rewritten as

$$H(s = j\omega) = \frac{1}{as^2 + bs + c} = \frac{\frac{1}{a}}{s^2 + 2\left(\frac{b}{2a}\right)s + \left[\frac{c}{a} - \left(\frac{b}{2a}\right)^2\right]} = \frac{\frac{4a}{b^2}}{\left(1 + j\frac{2a}{b}\omega\right)^2 + \left(\frac{2a}{b}\right)^2\left[\frac{c}{a} - \left(\frac{b}{2a}\right)^2\right]} \quad (31)$$

The magnitude-angular form of transfer function is

$$|H(j\omega)| = \frac{4a}{b^2} \frac{1}{\sqrt{\left(\frac{4a}{b}\omega\right)^2 + \left[1 - \left(\frac{2a}{b}\omega\right)^2 + \left(\frac{2a}{b}\right)^2\left[\frac{c}{a} - \left(\frac{b}{2a}\right)^2\right]\right]^2}}; \angle H(j\omega) = \arctan\left(\frac{-\frac{4a}{b}\omega}{1 - \left(\frac{2a}{b}\omega\right)^2 + \left(\frac{2a}{b}\right)^2\left[\frac{c}{a} - \left(\frac{b}{2a}\right)^2\right]}\right) \quad (32)$$

In critically damped case $\frac{c}{a} = \left(\frac{b}{2a}\right)^2$, the magnitude-angular form of transfer function is

$$|H(j\omega)| = \frac{4a}{b^2} \frac{1}{\sqrt{\left(\frac{4a}{b}\omega\right)^2 + \left(1 - \left(\frac{2a}{b}\omega\right)^2\right)^2}}; \angle H(j\omega) = \arctan\left(\frac{-\frac{4a}{b}\omega}{1 - \left(\frac{2a}{b}\omega\right)^2}\right) \quad (33)$$

At the cut-off angular frequency $\omega_{cut} = \frac{b}{2a}$, the magnitude-angular form of transfer function is

$$|H(j\omega)| = \frac{2a}{b^2}; \angle H(j\omega) = \arctan(-\infty) = -\frac{\pi}{2} \quad (34)$$

A.2. Self-loop function of second-order denominator complex function

From Eq. (13), the self-loop function is rewritten as

$$L(j\omega) = j\frac{4a}{b}\omega + \left(j\frac{2a}{b}\omega\right)^2 + \left(\frac{2a}{b}\right)^2 \left[\frac{c}{a} - \left(\frac{b}{2a}\right)^2\right] \quad (35)$$

The magnitude-angular form of self-loop function is

$$|L(j\omega)| = \sqrt{\left(\frac{4a}{b}\omega\right)^2 + \left(\left(\frac{2a}{b}\right)^2 \left[\frac{c}{a} - \left(\frac{b}{2a}\right)^2\right] - \left(\frac{2a}{b}\omega\right)^2\right)^2}; \angle L(j\omega) = \arctan\left(\frac{\frac{4a}{b}\omega}{\left(\frac{2a}{b}\right)^2 \left[\frac{c}{a} - \left(\frac{b}{2a}\right)^2\right] - \left(\frac{2a}{b}\omega\right)^2}\right) \quad (36)$$

The real-imaginary form of self-loop function is

$$\text{Re}\{L(j\omega)\} = \left(\frac{2a}{b}\right)^2 \left[\frac{c}{a} - \left(\frac{b}{2a}\right)^2\right] - \left(\frac{2a}{b}\omega\right)^2; \text{Im}\{L(j\omega)\} = \frac{4a}{b}\omega \quad (37)$$

In critically damped case $\frac{c}{a} = \left(\frac{b}{2a}\right)^2$, the self-loop function is

$$L(j\omega) = j\frac{4a}{b}\omega \left(1 + j\frac{a}{b}\omega\right) = \sqrt{\left(\frac{4a}{b}\omega\right)^2 + \left(\frac{2a}{b}\omega\right)^4} e^{j\arctan\left(\frac{2}{-\left(\frac{2a}{b}\omega\right)}\right)} \quad (38)$$

At the angular frequency $\omega = \frac{b}{a}$, the magnitude-angular form of self-loop function is

$$|L(j\omega)| = 4\sqrt{2}; \angle L(\omega) = \arctan(-1) = -45^\circ \quad (39)$$

The real-imaginary form of self-loop function is

$$\operatorname{Re}\{L(j\omega)\} = -4; \operatorname{Im}\{L(j\omega)\} = 4 \quad (40)$$

At the angular frequency $\omega_{cut} = \frac{b}{2a}$, the magnitude-angular form of self-loop function is

$$|L(j\omega)| = \sqrt{5}; \angle L(j\omega) = \arctan(-2) = -63.4^\circ \quad (41)$$

The real-imaginary form of self-loop function is

$$\operatorname{Re}\{L(j\omega)\} = -1; \operatorname{Im}\{L(j\omega)\} = 2 \quad (42)$$

At unity gain of the self-loop function, we have

$$|L(\omega_u)| = 1 \Rightarrow \left| \frac{4a}{b} \omega_u \sqrt{1 + \left(\frac{a}{b} \omega_u\right)^2} \right| = 1 \quad (43)$$

Solving Eq. (43), the angular frequency ω_u at unity gain is

$$\omega_u = \frac{b}{2a} \sqrt{\sqrt{5} - 2} \quad (44)$$

The relationship between the angular frequency ω_u and the cut-off angular frequency $\omega_{cut} = \frac{b}{2a}$ is

$$\omega_u = \omega_{cut} \sqrt{\sqrt{5} - 2} \Rightarrow \omega_{cut} = \frac{\omega_u}{\sqrt{\sqrt{5} - 2}} \quad (45)$$

At unity gain angular frequency $\omega_u = \frac{b}{2a} \sqrt{\sqrt{5} - 2}$, the magnitude-angular form of self-loop function is

$$|L(j\omega)| = 1; \angle L(j\omega) = \arctan\left(\frac{-2}{\sqrt{\sqrt{5} - 2}}\right) = -76.35^\circ \quad (46)$$

The real-imaginary form of self-loop function is

$$\operatorname{Re}\{L(j\omega)\} = 2 - \sqrt{5}; \operatorname{Im}\{L(j\omega)\} = 2\sqrt{\sqrt{5} - 2} \quad (47)$$

In underdamped case $\frac{c}{a} < \left(\frac{b}{2a}\right)^2$, the self-loop function is

$$L(j\omega) = j\frac{4a}{b}\omega - \left(j\frac{2a}{b}\omega\right)^2 - \left[\left(\frac{2a}{b}\right)^2 \left[\frac{c}{a} - \left(\frac{b}{2a}\right)^2\right]\right] \quad (48)$$

The magnitude-angular form of self-loop function is

$$|L(j\omega)| = \sqrt{\left(\frac{4a}{b}\omega\right)^2 + \left[-\left(\frac{2a}{b}\right)^2 \left[\frac{c}{a} - \left(\frac{b}{2a}\right)^2\right] - \left(\frac{2a}{b}\omega\right)^2\right]^2}; \angle L(j\omega) = \arctan\left(\frac{\frac{4a}{b}\omega}{-\left[\left(\frac{2a}{b}\right)^2 \left[\frac{c}{a} - \left(\frac{b}{2a}\right)^2\right] - \left(\frac{2a}{b}\omega\right)^2\right]}\right) \quad (49)$$

The real-imaginary form of self-loop function is

$$\text{Re}\{L(j\omega)\} = -\left[\left(\frac{2a}{b}\right)^2 \left[\frac{c}{a} - \left(\frac{b}{2a}\right)^2\right] - \left(\frac{2a}{b}\omega\right)^2\right]; \text{Im}\{L(j\omega)\} = \frac{4a}{b}\omega \quad (50)$$

At the angular frequency $\omega = \frac{b}{a}$, the magnitude-angular form of self-loop function is

$$|L(j\omega)| = \sqrt{(4)^2 + \left[-\left[\left(\frac{2a}{b}\right)^2 \left[\frac{c}{a} - \left(\frac{b}{2a}\right)^2\right] - (4)^2\right]\right]^2} > 4\sqrt{2}; \angle L(j\omega) = \arctan\left(\frac{4}{-\left[\left(\frac{2a}{b}\right)^2 \left[\frac{c}{a} - \left(\frac{b}{2a}\right)^2\right] - 4\right]}\right) < \arctan(-1) = -45^\circ \quad (51)$$

At the angular frequency $\omega_{cut} = \frac{b}{2a}$, the magnitude-angular form of self-loop function is

$$|L(j\omega)| = \sqrt{4 + \left[-\left[\left(\frac{2a}{b}\right)^2 \left[\frac{c}{a} - \left(\frac{b}{2a}\right)^2\right] - 1\right]\right]^2} > \sqrt{5}; \angle L(j\omega) = \arctan\left(\frac{2}{-\left[\left(\frac{2a}{b}\right)^2 \left[\frac{c}{a} - \left(\frac{b}{2a}\right)^2\right] - 1\right]}\right) < \arctan(-2) = -63.4^\circ \quad (52)$$

The real-imaginary form of self-loop function is

$$\text{Re}\{L(j\omega)\} = -\left[\left(\frac{2a}{b}\right)^2 \left[\frac{c}{a} - \left(\frac{b}{2a}\right)^2\right] - 4\right] < -4; \text{Im}\{L(j\omega)\} = 4 \quad (53)$$

At unity gain angular frequency $\omega_u = \frac{b}{2a}\sqrt{\sqrt{5}-2}$, the magnitude-angular form of self-loop function is

$$|L(j\omega)| = \sqrt{2(\sqrt{5}-2) + \left(-\left(\frac{2a}{b}\right)^2 \left[\frac{c}{a} - \left(\frac{b}{2a}\right)^2 \right] + 2 - \sqrt{5} \right)^2} > 1; \angle L(j\omega) = \arctan \left(\frac{2\sqrt{5}-2}{-\left(\frac{2a}{b}\right)^2 \left[\frac{c}{a} - \left(\frac{b}{2a}\right)^2 \right] - (\sqrt{5}-2)} \right) < \arctan \left(\frac{-2}{\sqrt{5}-2} \right) = -76.35^\circ \quad (54)$$

The real-imaginate form of self-loop function is

$$\operatorname{Re}\{L(j\omega)\} = -\left[\left(\frac{2a}{b}\right)^2 \left[\frac{c}{a} - \left(\frac{b}{2a}\right)^2 \right] + 2 - \sqrt{5} \right] > 2 - \sqrt{5}; \operatorname{Im}\{L(j\omega)\} = 2\sqrt{5}-2 \quad (55)$$

In overdamped case $\frac{c}{a} > \left(\frac{b}{2a}\right)^2$, the self-loop function is

$$L(j\omega) = j\frac{4a}{b}\omega - \left(j\frac{2a}{b}\omega \right)^2 + \left[\left(\frac{2a}{b}\right)^2 \left[\frac{c}{a} - \left(\frac{b}{2a}\right)^2 \right] \right] \quad (56)$$

The magnitude-angular form of self-loop function is

$$|L(j\omega)| = \sqrt{\left(\frac{4a}{b}\omega\right)^2 + \left(\left[\left(\frac{2a}{b}\right)^2 \left[\frac{c}{a} - \left(\frac{b}{2a}\right)^2 \right] - \left(\frac{2a}{b}\omega\right)^2 \right)^2} ; \angle L(j\omega) = \arctan \left(\frac{\frac{4a}{b}\omega}{\left[\left(\frac{2a}{b}\right)^2 \left[\frac{c}{a} - \left(\frac{b}{2a}\right)^2 \right] - \left(\frac{2a}{b}\omega\right)^2 \right]} \right) \quad (57)$$

The real-imaginate form of self-loop function is

$$\operatorname{Re}\{L(j\omega)\} = \left[\left(\frac{2a}{b}\right)^2 \left[\frac{c}{a} - \left(\frac{b}{2a}\right)^2 \right] - \left(\frac{2a}{b}\omega\right)^2 \right]; \operatorname{Im}\{L(j\omega)\} = \frac{4a}{b}\omega \quad (58)$$

At the angular frequency $\omega = \frac{b}{a}$, the magnitude-angular form of self-loop function is

$$|L(j\omega)| = \sqrt{(4)^2 + \left(\left[\left(\frac{2a}{b}\right)^2 \left[\frac{c}{a} - \left(\frac{b}{2a}\right)^2 \right] - (4)^2 \right)^2} < 4\sqrt{2}; \angle L(j\omega) = \arctan \left(\frac{4}{\left[\left(\frac{2a}{b}\right)^2 \left[\frac{c}{a} - \left(\frac{b}{2a}\right)^2 \right] - 4 \right]} \right) > \arctan(-1) = -45^\circ \quad (59)$$

The real-imaginate form of self-loop function is

$$\operatorname{Re}\{L(j\omega)\} = \left[\left(\frac{2a}{b}\right)^2 \left[\frac{c}{a} - \left(\frac{b}{2a}\right)^2 \right] - 4 \right] > -4; \operatorname{Im}\{L(j\omega)\} = 4 \quad (60)$$

At the angular frequency $\omega_{cut} = \frac{b}{2a}$, the magnitude-angular form of self-loop function is

$$|L(j\omega)| = \sqrt{4 + \left(\left(\frac{2a}{b} \right)^2 \left[\frac{c}{a} - \left(\frac{b}{2a} \right)^2 \right] - 1 \right)^2} < \sqrt{5}; \angle L(j\omega) = \arctan \left(\frac{2}{\left(\frac{2a}{b} \right)^2 \left[\frac{c}{a} - \left(\frac{b}{2a} \right)^2 \right] - 1} \right) > \arctan(-2) = -63.4^\circ \quad (61)$$

At unity gain angular frequency $\omega_u = \frac{b}{2a} \sqrt{\sqrt{5}-2}$, the magnitude-angular form of self-loop function is

$$|L(j\omega)| = \sqrt{2(\sqrt{5}-2) + \left(\left(\frac{2a}{b} \right)^2 \left[\frac{c}{a} - \left(\frac{b}{2a} \right)^2 \right] + 2 - \sqrt{5} \right)^2} < 1; \angle L(j\omega) = \arctan \left(\frac{2\sqrt{\sqrt{5}-2}}{\left(\frac{2a}{b} \right)^2 \left[\frac{c}{a} - \left(\frac{b}{2a} \right)^2 \right] - (\sqrt{5}-2)} \right) > \arctan \left(\frac{-2}{\sqrt{\sqrt{5}-2}} \right) = -76.35^\circ \quad (62)$$

The real-imaginary form of self-loop function is

$$\text{Re}\{L(j\omega)\} = \left(\frac{2a}{b} \right)^2 \left[\frac{c}{a} - \left(\frac{b}{2a} \right)^2 \right] - 1 > -1; \text{Im}\{L(j\omega)\} = 2 \quad (63)$$

A.3. Classical analysis of power stage

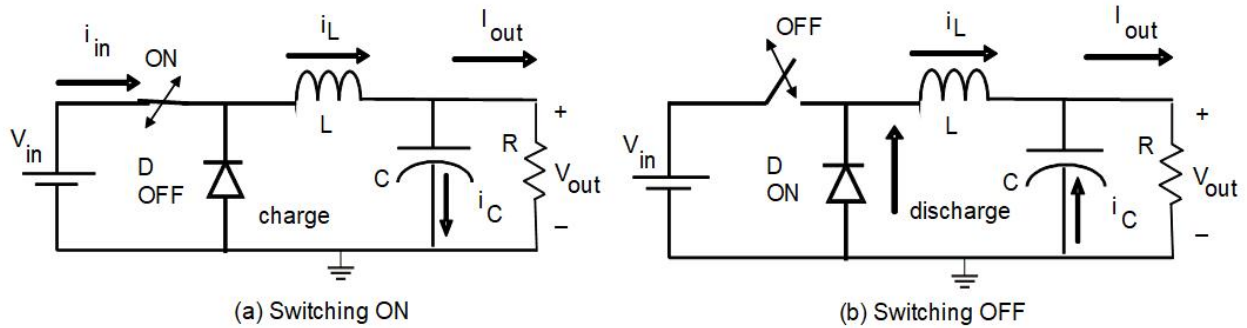


Fig. 16. Circuits of Figure 5.

As the switch is turned ON (or capacitor charges) as in Fig. 16 (a), apply the Kirchoff current law at the output node

$$i_L(t) = I_{out}(t) + i_C(t) \quad (64)$$

Here, the currents of each branch are given by

$$V_{out}(t) = \frac{Q(t)}{C}; I_{out}(t) = \frac{V_{out}(t)}{R}; i_C(t) = C \frac{d(V_{out}(t))}{dt}; i_L(t) = \frac{1}{L} \int_0^{T_{ON}} (V_{in} - V_{out}(t)) dt \quad (65)$$

Then, Eq. (64) is rewritten as

$$\frac{V_{out}(t)}{R} + C \frac{dV_{out}(t)}{dt} = \frac{1}{L} \int_0^{T_{ON}} (V_{in} - V_{out}(t)) dt \quad (66)$$

Then, simplify the Eq. (66) as

$$\frac{V_{out}(t)}{R} + \frac{1}{L} \int_0^{T_{ON}} V_{out}(t) dt + C \frac{dV_{out}(t)}{dt} = \frac{1}{L} \int_0^{T_{ON}} V_{in} dt \quad (67)$$

Assume that the initial voltage of the capacitor is given by a constant value. Apply the differential mathematics approach for Eq. (67)

$$\frac{1}{R} \frac{dV_{out}(t)}{dt} + \frac{V_{out}(t)}{L} + C \frac{d^2V_{out}(t)}{dt^2} = 0 \quad (68)$$

Then, the simplified form of Eq. (68) is expressed as

$$\frac{d^2V_{out}(t)}{dt^2} + \frac{1}{RC} \frac{dV_{out}(t)}{dt} + \frac{V_{out}(t)}{LC} = 0 \quad (69)$$

Suppose that the wave function of the output voltage is $V_{out}(t) = Ae^{st} = A_1e^{s_1t} + A_2e^{s_2t}$

$$\frac{d^2(Ae^{st})}{dt^2} + \frac{1}{RC} \frac{d(Ae^{st})}{dt} + \frac{(Ae^{st})}{LC} = 0 \quad (70)$$

Let us rewrite Eq. (70) in a short form

$$s^2 + \frac{1}{RC}s + \frac{1}{LC} = 0 \quad (71)$$

Solve Eq. (71), the values of s are defined by

$$s_1 = -\frac{1}{2RC} + \sqrt{\left(\frac{1}{2RC}\right)^2 - \frac{1}{LC}} \quad \vee \quad s_2 = -\frac{1}{2RC} - \sqrt{\left(\frac{1}{2RC}\right)^2 - \frac{1}{LC}} \quad (72)$$

Let us define $\omega_{2RC} = \frac{1}{2RC}$; $\omega_{LC} = \frac{1}{\sqrt{LC}}$; the wave function of the output voltage is rewritten by

$$V_{charge}(t) = A_{ch1} e^{\left(-\omega_{2RC} + \sqrt{(\omega_{2RC})^2 - \omega_{LC}^2}\right)t} + A_{ch2} e^{\left(-\omega_{2RC} - \sqrt{(\omega_{2RC})^2 - \omega_{LC}^2}\right)t} \quad (73)$$

The charge energy of the capacitor makes the current direction of energy at the output node change when the switch is turned OFF (or capacitor discharge). Besides, this energy also turns ON the diode. In this case, the current direction which goes pass the inductor is not changed. So, apply the Kirchoff's node rule at the output node

$$I_{out}(t) = i_L(t) + i_C(t) \quad (74)$$

In the duty OFF of the switching control signal, this energy is distributed on the inductor, the diode, and the resistor. The energy which is distributed on the resistor is always the same the voltage level of the capacitor. Here, the currents of each branch are given by

$$V_{dis}(t) = \frac{Q(t)}{C}; I_{out}(t) = \frac{V_{dis}(t)}{R}; i_C(t) = C \frac{d(V_{dis}(t))}{dt}; i_L(t) = \frac{1}{L} \int_{T_{ON}}^{T_{OFF}} (V_{dis}(t) - V_{diode}) dt \quad (75)$$

Then, Eq. (74) is rewritten as

$$\frac{V_{dis}(t)}{R} = C \frac{dV_{dis}(t)}{dt} + \frac{1}{L} \int_{T_{ON}}^{T_{OFF}} (V_{dis}(t) - V_{diode}) dt \quad (76)$$

Here, the simplified form of Eq. (76) is converted as

$$C \frac{dV_{dis}(t)}{dt} - \frac{V_{dis}(t)}{R} + \frac{1}{L} \int_{T_{ON}}^{T_{OFF}} V_{dis}(t) dt = \frac{1}{L} \int_{T_{ON}}^{T_{OFF}} V_{diode} dt \quad (77)$$

In all the time of duty OFF, the energy passes over the diode is a constant energy. Apply the differential mathematics approach for Eq. (77)

$$C \frac{dV_{dis}(t)}{dt} - \frac{V_{dis}(t)}{R} + \frac{1}{L} \int_{T_{ON}}^{T_{OFF}} V_{dis}(t) dt = 0 \quad (78)$$

Assume that the initial voltage of the capacitor is given by a constant value which is equal to the value of the charge voltage; the simplified form of Eq. (78) is expressed as

$$\frac{d^2 V_{dis}(t)}{dt^2} - \frac{1}{RC} \frac{dV_{dis}(t)}{dt} + \frac{V_{dis}(t)}{LC} = 0 \quad (79)$$

Suppose that the discharge voltage is $V_{dis}(t) = A_{dis} e^{st} = A_3 e^{s_{dis1}t} + A_3 e^{s_{dis2}t}$;

$$\frac{d^2 (A_{dis} e^{st})}{dt^2} - \frac{1}{RC} \frac{d(A_{dis} e^{st})}{dt} + \frac{(A_{dis} e^{st})}{LC} = 0 \quad (80)$$

Let us rewrite Eq. (80) in a short form

$$s^2 - \frac{1}{RC}s + \frac{1}{LC} = 0 \quad (81)$$

Solving Eq. (81), the values of s are defined by

$$s_{dis1} = \frac{1}{2RC} + \sqrt{\left(\frac{1}{2RC}\right)^2 - \frac{1}{LC}} \quad \vee \quad s_{dis2} = \frac{1}{2RC} - \sqrt{\left(\frac{1}{2RC}\right)^2 - \frac{1}{LC}} \quad (82)$$

Let us define $\omega_{2RC} = \frac{1}{2RC}$; $\omega_{LC} = \frac{1}{\sqrt{LC}}$; the wave function of the output voltage is rewritten by

$$V_{discharge}(t) = A_{dis1} e^{\left(\omega_{2RC} + \sqrt{(\omega_{2RC})^2 - \omega_{LC}^2}\right)t} + A_{dis2} e^{\left(\omega_{2RC} - \sqrt{(\omega_{2RC})^2 - \omega_{LC}^2}\right)t} \quad (83)$$

A.4. Frequency response of power stage of buck converter

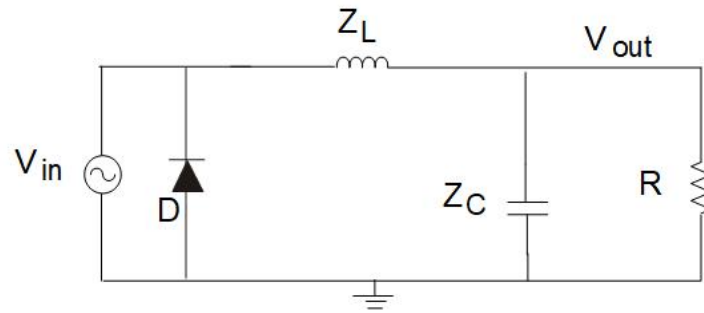


Fig. 17. Circuit of Figure 6(a).

Apply the widened superposition at output node

$$V_{out} \left(\frac{1}{R} + \frac{1}{Z_C} + \frac{1}{Z_L} \right) = \frac{V_{in}}{Z_L} \quad (84)$$

Then, the transfer function is

$$H(s) = \frac{V_{out}}{V_{in}} = \frac{1}{1 + Z_L \left(\frac{1}{R} + \frac{1}{Z_C} \right)} = \frac{1}{LCs^2 + s \frac{L}{R} + 1} = \frac{\left(\frac{1}{LC} \right) / \left(\frac{1}{2RC} \right)^2}{\left[(2RC)^2 s^2 + 2s(2RC) + 1 \right] + (2RC)^2 \left[\frac{1}{LC} - \left(\frac{1}{2RC} \right)^2 \right]} \quad (85)$$

A.5. Overshoot improvement of RLC network

By applying the superposition principle at the output node, the voltage relationships between input sources and the output sources are expressed in Eq. (86).

$$V_{out} \left(\frac{1}{Z_{L1}} + \frac{1}{Z_{C1}} + \frac{1}{R_1} + \frac{1}{R_2 + Z_{L2} + Z_{C2}} \right) = \frac{V_{in}}{Z_{L1}} \quad (86)$$

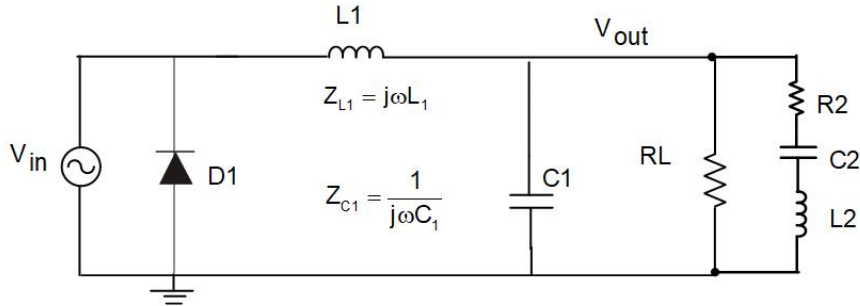


Fig. 18. Circuit of Figure 9(a).

The transfer function of this network is written as Eq. (87).

$$H = \frac{V_{out}}{V_{in}} = \frac{1}{1 + j\omega \frac{L_1}{R_1} + (j\omega)^2 \left(L_1 C_1 + \frac{C_2 L_1}{L_2 C_2 (j\omega)^2 + j\omega C_2 R_2 + 1} \right)} \quad (87)$$

A.6. Adaptive feedback loop

Apply the superposition principle at the reference voltage node

$$V_{ref} \left(\frac{1}{Z_{C1}} + \frac{1}{R_1} + \frac{1}{Z_{C2} + R_2} \right) = \frac{V_{cont}}{Z_{C2} + R_2} + V_{out} \left(\frac{1}{Z_{C1}} + \frac{1}{R_1} \right) \quad (88)$$

After simplifying Eq. (88), the control voltage is expressed as:

$$V_{cont} = V_{ref} + \frac{(Z_{C1} + R_1)(Z_{C2} + R_2)}{Z_{C1} R_1} (V_{ref} - V_{out}) \quad (89)$$

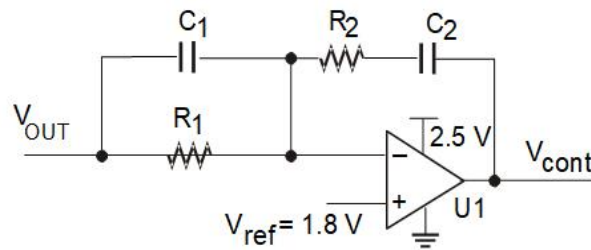


Fig. 19. Circuit of Figure 12.